Early Paleoproterozoic Metallogenic Explosion in North China Craton

12

Haoshu Tang, Yanjing Chen, Kaiyue Li, Weiyu Chen, Xiaoqing Zhu, Kunyue Ling, and Xiaohui Sun

Abstract

This chapter compiles the geology and geochronology of numerous ores, including graphite, phosphorite, the Lake Superior type BIFs, marble, boron, magnesite, and lead-zinc deposits, hosted in 2.5–1.8 Ga stata from the North China Craton (NCC) and elsewhere, and thereby provides insights into understanding the mineralization of the early Paleoproterozoic metallogenic explosion in NCC. These mineralized records, accompanied with the blooms of biological photosynthesis (indicated by graphite, phosphorite deposits, organics in black shale), suggested different mineralizations, which responded to different stages of dramatic Earth's environmental changes characteristic of the Great Oxidation Event (GOE). These changes includes that the early-stage hydrosphere oxidation (2.5–2.3 Ga), indicated by numerous development of the Lake Superior type BIFs; through the turnpoint from hydrosphere to atmosphere oxidation (2.3–2.25 Ga), indicated by the 2.29–2.25 Ga Huronnian Glaciation Event (HGE) and devoid of Rand-type Au–U deposits, to the late-stage atmospheric oxygenation, followed by 2.25–1.8 Ga sediments of thick-bedded carbonates strata and related deposits (e.g., marble, magnesite, boron, and lead-zinc deposits), the 2.25–1.95 Ga red beds, 2.22–2.06 Ga $\delta^{13}C_{carb}$ positive excursion (Lomagundi/Jatulian Event), as well as the prevail of black shales at 2.0–1.7 Ga and disappear of BIFs at ca. 1.8 Ga.

Keywords

Mineralization • Great Oxidation Event (GOE) • Early paleoproterozoic living bloom • Ph of seawater • Earth's environmental changes

H. Tang (✉) · X. Zhu · K. Ling · X. Sun
State Key Laboratory of Ore Deposit Geochemistry,
Institute of Geochemistry, Chinese Academy of Sciences,
99 Linchengxi Roud, Guiyang, 550081, China
e-mail: tanghaoshu@163.com

Y. Chen (✉) · K. Li · W. Chen
Key Laboratory of Crustal and Orogenic Evolution,
Peking University, Beijing, 100871, China
e-mail: yjchen@pku.edu.cn

X. Sun
School of Earth Science and Resources,
Chang'an University, Xi'an, 710054, China

12.1 Introduction

The Siderian/Rhyacian transition (2.3 Ga) witnessed dramatic environmental changes (e.g., Chen 1990; Chen and Su 1998; Holland 2009; Chen and Tang 2016, in Chap. 11; and references therein) in Earth's history characteristic of the Great Oxidation Event (GOE), which mainly occurred in the period of 2.5–2.2 Ga and includes the pre-2.3 Ga earlier hydrosphere oxidation stage and the post-2.3 Ga later atmosphere oxygenation stage (Tang and Chen 2013). The tectonic processes and global environmental changes during the Palaeoproterozoic from 2.5 to 1.6 Ga have been the focus of numerous studies in the past decades (e.g., Chen 1990, 1996b; Bekker et al. 2010; Holland 2009; Konhauser et al. 2009, 2011; Lyons and Reinhard 2009; Young 2012, 2013; Zhai and Santosh 2013; Zheng et al. 2013; Li et al. 2015a; and references therein). Particularly in the early paleoproterozoic (2.3–1.8 Ga) period, voluminous red beds, evaporites, stromatolite-bearing carbonates (Chen 1990; Melezhik et al. 1999a; Bekker et al. 2006; Tang et al. 2009a, b, c, 2011, 2013a; Lai et al. 2012), Superior type banded iron formations (Huston and Logan 2004; Zhao 2010; and references therein), phosphate, graphite (Melezhik et al. 1999b; Chen et al. 2000a), lead-zinc, uranium, talcum, boron, and magnesite deposits (e.g., the Dashiqiao magnesite belt deposits; Tang et al. 2013b) evolved rapidly. However, there are several questions remaining unanswered including whether these Palaeoproterozoic stratum record the GOE, and whether the sedimentary–metamorphic deposits are genetically related to the GOE. A key to these problems is important in understanding the Precambrian evolution and mineralizations during the early Earth history but have rarely studies (Chen 1996b; Chen et al. 2000a; Tang et al. 2009a, b, c, 2013a, b).

The North China Craton (NCC) is an Early Precambrian continental block with widespread early Palaeoproterozoic strata (see Zhai et al. 2010; Zhai and Santosh 2011; Zheng et al. 2013), which hosts numerous ore deposits. In this study, therefore, we compile early paleoproterozoic ores or host rock geology and geochronological data obtained for the NCC (Table 12.1; Figs. 12.1, 12.2), and evaluate the scientific problems related to the GOE, and the implications of the mineralization in the NCC.

12.2 Early Paleoproterozoic Metallogenic Explosion and Records in NCC

Many aspects of the Earth's surficial system changed dramatically at about 2300 Ma (for detail see Chap. 11), suggesting the occurrence of a catastrophe in geological environment at about 2300 Ma. What is responsible for the changes in the Earth's surficial environment? How can we appeal this discovery to understand the Precambrian geological evolution, and mineralization of ore deposits? Every item of those changes includes lots of detailed data, which makes us only introduce few sections here instead of all of them.

12.2.1 The First Episode of Worldwide Graphite Resources and Record in NCC

Schopf (1977) pointed out that if sporadic evidences of life were preserved in the Archaeozoic, the data about paleontologic activities would increase greatly in the Proterozoic. Schopf (1977) further pointed out that the reports on the threadlike and ultramicro fossils as the evidences of life were not reliable, more convincing evidences in the Precambrian were stromatolites. It has been reported that the Archaeozoic stromatolites were discovered in four areas, and only the stromatolites in limestones of the Bulawayan Group in the southern part of Africa are more widely accepted, which suggest that organic activities were extremely weak before 2300 Ma. Researches of life in the Archaeozoic have made great development since 1976 (Awramik et al. 1983), however, convincing evidences of life are still deficient. The evidences of life have been rapidly accumulated since 2300 Ma (Knoll et al. 1988; Schopf 1977), and stromatolites (especially the stromatolites bearing blue-green algae) were extensively developed in the world (Melezhik et al. 1997a, b). Ferrobacteria fossils have been discovered in the iron ores in Krivoy Rog, Kazakstan, and Siberia areas, and the ages of these strata are confined to the period of 2300–1900 Ma. Carbonate rocks (2300–2000 Ma) in Baihai Group had been interacting with bacteria during the precipitating, and in Kola peninsula, carbonatized germ microfossils have been reported in the calcite grains in some marbles (Melezhik et al. 1997a, 1999a; and references therein). Moreover, both diversity of taxa and abundance of Palaeoproterozoic stromatolites are sharply increased (Melezhik et al. 1997a). Karelian shungite even gave an indication of 2.0-Ga-old metamorphosed oil-shale and generation of petroleum (Melezhik et al. 1999a).

Well preserved threadlike blue-green algae, medusoid fossils have been discovered in the strata during Huronian period in Ontario area, and Gruneria binabikin have been discovered in the Biwabik and Gunflint iron formations in Minnesota and Ontario areas, respectively (Cloud and Semikhatov 1969). All kinds of stromatolites, such as *Katernia africana*, were reported to be in the dolomite series of 2000 Ma in north Cape Province of the southern part of Africa, and in the Transvaal dolomite series, other stromatolites (2300–1950 Ma) were also found (Cloud and Semikhatov 1969). Hamersley and Uru Groups abounded

Table 12.1 The geology and geochronology of graphite, phosphorite, the Lake Superior type BIFs, marble, boron, magnesite, and lead-zinc deposits hosted in ca 2.5–1.8 Ga stata from the North China Craton (NCC)

No.	Country	Locality or host rock assemblage	Characteristics of ores or host rocks	Age of ores or host rocks	References
Graphite ore					
1	Jilin, China	Ji'an city; Ji'an Group, Huangchagou Fm	Graphite biotite granulite; C% = 2.8–6.67 %	1916–1906	Zhang and Liu (2014), Wu et al. (2011)
2	Liaoning, China	Huanren county; Taizihe-Hunjiang trap; Liaohe Group,Gaojiayu Fm	Graphite tremolite monzogranulite, graphite tremolite; C% = 9.75 %	2200–1860	Wu and Qu (1994)
3	Liaoning, China	Heigou town; Liaohe Group	Graphite tremolite granulite; graphite tremolite; C% = 4.62-10.41 %	2191–1850	Sun et al. (1995)
4	Shandong, China	Nanshu town, Laixi city; Jingshan Group	Garnet plagioclase gneiss type, diopsidite type, marble type	2100–1900	Zhang et al. (2014b), Chen et al. (2000), Liu et al. (2011), Liu et al. (2015b)
5	Shandong, China	Jingcun deposit, Mingcun town, Pingdu city; Douya Fm., Jingshan Group	Graphite biotite monzogneiss, biotite granulite, diopside marble; C% = 2.5–5 %	2100-1900	Li (2014), Liu et al. (2011), Liu et al. (2015b)
6	Shandong, China	Zhangshe deposit, east Xishiling country, Zhangshe town, Pingdu city; Douya Fm., Jingshan Group	8.534 × 10⁵tons, graphite diopside plagiogneiss, graphite biotite plagiogneiss, coarse grain graphitegranulite biotite and muscovite plagiogneiss	2100–1900	Wan et al. (2006), Liu et al. (2011), Liu et al. (2015a), Liu et al. (2015b), Li et al. unpublicated; Tang et al. unpublicated
7	Henan, China	Neixiang county; Wuyangshan deposit; Yanlinggou Fm; Shicaogou Fm., Qinling Group	Plagiogneiss type; marble type; broken crack rock type; C% = 3–25 %	2226–1987	Zhang (2013)
8	Henan, China	Beizi deposit, Lushan county, Henan; Shuidigou Fm., Lushan (Upper Taihua) Group	Graphite biotite plagiogneiss, graphite diopside plagiogneiss, graphite plagiogneiss, graphite tremolite plagiogneiss; layered, stratoid, lentoid, 58 ore bodys; 940–2370 m in length, 2.04–22.88 m in thickness, crystal graphite deposit; C% = 3–25 %	2250–1850	Wan et al. (2006), Yang (2008), Diwu et al. (2010), Wang and Xue (2010), Shen and Song (2014), Li et al. (2015b)
9	Hebei, China	Kangbao county, Chicheng county; Hongqiyingzi Group	Graphite-bearing granulite, graphite-bearing garnet amphibole biotite plagioclase gneiss; C% = 2.57–4.57 %	2350–2330	Fu (2014)
10	Inner Mongolia, China	Huangtuyao county; Huai'an terrain	Gray gneiss, metasedimentary rocks (khondalites) and mafic (high-pressure) granulites	2150–1850	Zhang et al. (2014a), Yang et al. (2014)
11	Inner Mongolia, China	Jining city, Zhuozi county; Jijing Group	Graphite gneiss, biotite graphite plagioclase gneiss; C% = 2–8 %	~2300	Liu et al. (1989)
Phosphorite deposits					
12	North Korea	Chengjin Fm, Macheonryeong Series	Equivalent to the Laoling Group in South Jilin	2100–1700	Li et al. (1994)

(continued)

Table 12.1 (continued)

No.	Country	Locality or host rock assemblage	Characteristics of ores or host rocks	Age of ores or host rocks	References
13	North Korea	Yongrou; Hanchuan; Napu	Kondalite series, Nangnim Group, equivalent to the Kuandian Group in South Jilin	2035–1885	Li et al. (1994), Wu et al. (2007a, b), Meng et al. (2013, 2014)
14	S Jilin, China	Hunjiang (Baishan)	P_2O_5 = 14.00 %, Laoling Group	2100–1950	Li et al. (1994), Liu et al. (2015a)
15	S Jilin, China	Shangqinggou, Ji'an	P_2O_5 = 3.64 %, Ji'an Group	2100–1950	Li et al. (1994), Liu et al. (2015a)
16	S Jilin, China	Banshigou; Yangmuchuan, Kuandian	Zhuanmiao Fm. of the Kuandian Gp., Coexist with boron deposits	2035–1885	Zhu (1982), Zhang (1984), Li et al. (1994), Meng et al. (2013, 2014)
17	E Liaoning, China	Tianshui, Langzishan, Dashiqiao, Zhenzhumen and Luotun deposits, hosted in the Gaojiayu Fm. of the Liaohe Gp	7 million tons with P_2O_5 = 12.98 % (Tianshui), associations of P, P-B-REE, P-Mg, P-V, and P-Fe respectively	2050–1950	Li et al. (1994), Liu et al. (2015a)
18	W Liaoning, China	Wulanwusu, Jianping; Gongguanyingzi, Fuxin	P_2O_5 > 4 %. Xiaotazigou Fm. of Jianping Gp. khondalite series	2450–1900; ca. 2250	Zhu (1982), Li et al. (1994), Lu et al. (1996)
19	Shandong, China	Yexian (Laizhou city, including three occurrences), Jiaodong	Jingshan and Fenzishan Groups	2100–1900	Ji and Chen (1990), Hu et al. (1997), Wan et al. (2006), Liu et al. (2015a, 2015b)
20	Hebei, China	Zhaobinggou, Fengning	P_2O_5 = 5.25 %. Coexist with V, Fe. Baimiao Fm. of Dantazi Gp. khondalite Series	2.55–2.45 Ga	Zhu (1982), Li et al. (1994), Xia and Wei (2005), Liu et al. (2007a)
21	Inner Mongolia, China	Hohhot-Jining-Fengzhen-Hunyuanyao	P_2O_5 > 4 %. Huangtuyao khondalite Series. Coexist with graphite, Mn, Fe etc.	<2316 or 2270–1892; 2150–1850	Zhu (1982), Guo et al. (1994), Wu et al. (1998, 2006), Yang et al. (2014), Zhang et al. (2014a)
22	Wutaishan of Shanxi, China	Baijiashan and several other occurrences of Dongjiao type	P_2O_5 = 13.95 %, Biancun Formation in Dongye Subgroup of Hutuo Group	2200–1820	Zhao (1982), Goodwin (1991), Li et al. (1994), Widle et al. (2004), Wan et al. (2010b), Du et al. (2015)
23	Zhongtiaoshan, Shanxi	Danshanshi Group		1848–1800	Li et al. (1994), Liu et al. (2012)
24	Henan, China	Huayu, Songshan	Huayu Formation, Songshan Group	2337 ± 23 –2000	Hu (1988), Li et al. (1994), Diwu et al. (2008), Wan et al. (2009)
Lake Superior type BIFs					
25	Shandong, China	Changyi-Anqiu iron-ore belt, Xiaosong Fm., Fengzishan Group, Jiaobei terrain	~20 middle/little size ore deposits, shallow-water, high-energy environment; 1.253 × 10^8 tons, Fe^T = 29.2 %	2240–2193	Lan et al. (2012), (2014a, b), (2015b)
26	Anhui, China	Huoqiu iron-ore field, Zhouji and Chongxingji towns, north-west Hefei city, Anhui Province	>17.12 × 10^8 tons, Zhouji and Wuji Fm., Huoqiu Group	2700–1850	Wan et al. (2010a), Yang et al. (2012), Liu and Yang (2013), (2015)

(continued)

Table 12.1 (continued)

No.	Country	Locality or host rock assemblage	Characteristics of ores or host rocks	Age of ores or host rocks	References
27	Henan, China	Wuyang-Xingcai iron ore-field, Henan	Tieshan (2.47×10^8 tons), Jingshanshi (2.24×10^8 tons), layered, stratoid, lentoid, hosted in the No. 2–3 Section of Tieshanmiao Fm. (overlying on the Zhao'anzhuang Fm.), Upper Taihua Group	2250–1850	Wan et al. (2006), Yang (2008), Diwu et al. (2010), Wang and Xue (2010), Li and Zhang (2011), Li et al. (2012), Li et al. (2013b), Liu et al. 2014, Shen and Song (2014), Li et al. (2015b)
28	Shanxi, China	Yuanjiachun,Lvliang, Shanxi	>1.2 billion tons, three occurrences, hosted in metasedimentary rock succession of the 840–1200 mYuanjiacun Formation, lower Lüliang Group	2380–2210	Zhu and Zhang (1987), Shen et al. (2010), Zhang et al. (2012), Wang et al.(2015a, b, c)
Boron deposits					
29	Jilin, China	Ji'an county; Ji'an Group	Serpentinite; Biotite granulite; Marble	2100–1950	Wang and Han (1989), Feng et al. (2008), Liu et al. (2015a)
30	Liaoning, China	Kuandian county, Zhuanmiao deposit, Li'eryu Fm., Liaohe Group	large-size Ludwigite deposit, hosted in banding magnesite-marbles or near-banding serpentinized Mg-olivine rocks, volcanic–sedimentary formations; serpentined marble; $B_2O_3 = 10.52$–16.02 %	2170–1869	Hu et al. (2014), Xie et al. (2015)
31	Liaoning, China	Fengcheng city; Kuandian county; Liaohe Group	magnesium peridotite; serpentinization peridotite; Pyroclastic rock; $B_2O_3 = 0.51$–36.97 %	2191–1829	Liu et al. (2005a), Wang et al. (2008)
32	Liaoning, China	Wengquangou deposit, Fengcheng city; Li'eryu Fm., Liaohe Group	large-size Ludwigite deposit, hosted in banding magnesite-marbles or near-banding serpentinized Mg-silicate rocks, biotite-granulite; plagio-leucogranulitite; amphibolite; $B_2O_3 = 3.98$–11.94 %	2050–1950	Peng et al. (1998), Wen and Teng (2014), Liu et al. (2015a)
33	Liaoning, China	Houxianyu deposit, Yingkou city; Li'eryu Fm., Liaohe Group	large-size szaibelyite deposit, hosted in banding magnesite-marbles or near-banding serpentinized Ultra-magnesium peridotite, biotite granulite, tourmaline rock; $B_2O_3 = 17.61$–41.51 %	2050-1950	Jiang et al. (1997), Wang et al. (2006), Tang et al. (2009a), Liu et al. (2015a)
34	Liaoning, China	Dashiqiao deposit, Yingkou city; Li'eryu Fm., Liaohe Group	Serpentined marble, granulite, tourmaline-granulite	2050–1950	Luo et al. (2004), Liu et al. (2005b, 2015a)
Magnesite deposits					
35	Liaoning, China	Dashiqiao magnesite belt, including the Shengshuishi, Qingshanhuai, Shuiquan, Huaziyu, Pailou, Jinjiabao, Xiafangsheng and Fanjiabaozi deposits, Dashiqiao and Haicheng countries, Dashiqiao Fm., Liaohe Group	Controlled by the third member of the Dashiqiao Fm. dolomites with bedded or lens-type occurrence, and comprise an important part of the Dashiqiao strata; proven reserve ca. 2.987 billion tons	2050–1950	Jiang et al. (2004), Tang et al. (2009b, c, 2013a), Liu et al. (2015a)

Table 12.1 (continued)

No.	Country	Locality or host rock assemblage	Characteristics of ores or host rocks	Age of ores or host rocks	References
36	Shandong, China	Laizhou city, Jiaodong, Fenzishan Group	ca. 0.18 billion tons, seven occurrences, hosted in the Fengzishan Group	2100–1900	Wan et al. (2006), Liu et al. (2015a), Liu et al. 2015, Tang et al. unpublicated
Pb–Zn deposits					
37	Liaoning, China	Tieling city, Fanhe Basin, Liaobei terrain, intermediate-acidic volcanic rocks, feldspathic quartzarenite and carbonates	$>57.3 \times 10^4$ tons, stromatolitic clastic sediments, shales, and limestones and dolomites, Guanmenshan Fm., North Liaohe Group	2330–2060	Rui et al. (1991), Tang et al. (2008; 2011)
38	Liaoning, China	Qingchengzi Pb–Zn (Ag–Au) ore-field, East Liaoning	stromatolitic clastic sediments, shales, and limestones and dolomites, Pb–Zn $> 150 \times 10^4$ tons hosted in Langzishan and Dashiqiao Fms., Liaohe Group; Au > 200 tons, and Ag > 1100 tons, hosted in Dashiqiao and Gaixian Fms., Liaohe Group	2050–1950	Jiang (1988), Jiang and Wei (1989), Chen (2002), Duan et al. (2012), Liu et al. (2013), Liu et al. (2015a)
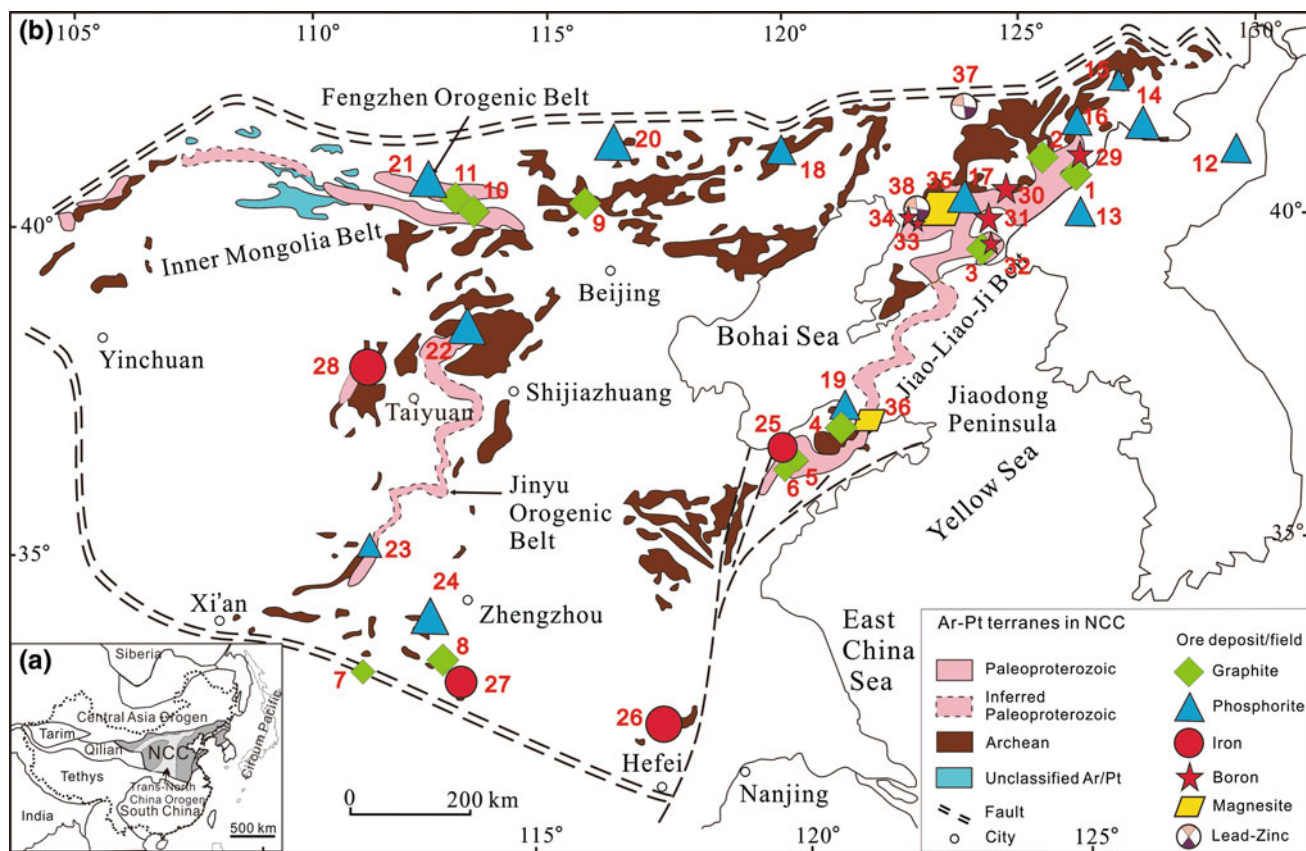
Fig. 12.1 The distribution and size of the part early Paleoproterozoic sedimentary ores in North China Craton (NCC). See Table 12.1 for the number of ore deposit/belt and references source.

Archaean-Palaeoproterozoic terranes of the NCC (modified after Zhai and Santosh 2011). Ar/Pt = Archaean/Proterozoic

with algae fossils (Knoll et al. 1988). In the Onega Group, and locally in the Segozero Group, large amount of various stromatolitic bioherms, and in some cases, oncolites are found (Salop 1977). Furthermore, those stromatolite-bearing strata are often associated with graphite deposits, and carbon isotopic researches suggest that graphite deposits are organogenic. For instances, carbon isotopes of graphite deposits in 2.5–2.2 Ga Eastern Ghats Mobile Belt, Orissa, India, are −26.6 to −2.4 ‰ (Sanyal et al. 2009), in ∼1.9 Ga Kerala Khondalite Belt (KKB) of southern India, are −18.06 to −17.87 ‰ (Cenki et al. 2004; Satish-Kumar et al. 2011); and in 2.45–2.3 Ga Sargur Area, Western Dharwar Craton, India, are −25.2 to −20.5 ‰ (Maibam et al. 2015).

In NCC, Liaohe, Songshan, Hutuo, and Feizishan Groups also abound with stromatolites (Cao et al. 1982; Cao 2003; Cao and Yuan 2003, 2009; Gao et al. 2009; Lai et al. 2012). Many graphite deposits are hosted in these 2.3–1.85 Ga early paleoproterozoic strata (Figs. 12.1, 12.2; Table 12.1). Carbon isotope researches suggest that Lushan of Henan (Chen and Deng 1993), Nanshu of Jiaodong (Lan 1981) and

Xinhe of the Inner Mongolia graphite deposits are all organogenic, organic activities are very intense (Chen et al. 2000; Zhang 2013; Yang et al. 2014).
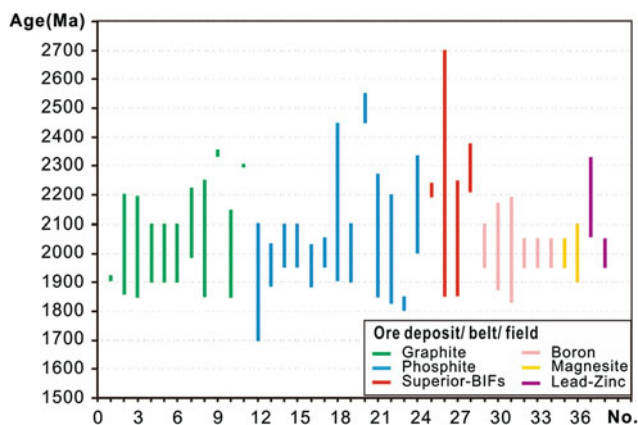
Fig. 12.2 The ages of the part early Paleoproterozoic sedimentary ores in North China Craton (NCC). See Table 12.1 for the number of ore deposit/belt and references source

In sum, sudden increase of organic activities at 2300 Ma resulted in a leap in the living beings evolution.

12.2.2 The First Period of Global Phosphorites and Record in NCC

"As recently as 1962, Geijer argued that there was an almost total absence of phosphorites in the Precambrian" (recited from Cook and Mcelhinny 1979). Davidson (1963), Cook and Mcelhinny (1979) documented the Precambrian phosphorites (including Archean) and denied Geijer's view. However, Windley (1980, 1984) pointed out that "phosphorite are phosphorus-rich sedimentary rocks that did not form in the Archean; minor phosphorites began to appear in the early Proterozoic, but major deposits not until the late Proterozoic".

Based on statistics of phosphorites in NCC (Table 12.1), all the authors indicated that Paleoproterozoic phosphorites and significant phosphorus deposits are documented widespread in the strata formed during 2500–1850 Ma (Fig. 12.2).

In China, phosphorites also occurred as the Dongjiao-type phosphorus deposits in the Songshan, Hutuo, and Liaohe Groups (Zhao 1982), which are Paleoproterozoic cratonic sediments on the NCC and experienced low-grade metamorphism at about 2100–1850 Ma.

It should be emphasized that, in the NCC (including North Korea) and its adjacent Jiamus Block, a lot of significant phosphorus deposits have been found in Khondalite series with age of 2300–1900 Ma (Figs. 12.1, 12.2; Table 12.1). The Shichang phosphorus deposit of Heilongjiang Province is located in the Paleoproterozoic Mashan Group, the Jiamus block, whose P_2O_5 content is 5 % in average (Liu 1988; Lu et al. 1996). Three phosphorus deposits have been found between 2100 and 1900 Ma Jingshan Group (Hu et al. 1997; Wan et al. 2006; Xie et al. 2014; Liu et al. 2015a), Yexian country, Shandong province (Ji and Chen 1990). The 2450–1900 Ma Zhaobinggou phosphorus deposit (Zhu 1982; Li et al. 1994; Xia and Wei 2005) occurs in the Baimiaozi Formation of 2.55–2.45 Ga Dantazi Group (Liu et al. 2007a, b) in Hebei Province. The Wulawusu phosphorus deposit is located in the Jianping Group in the west of Liaoning Province (Li et al. 1994). The borate-phosphorite formation was found paragenetic with marbles in 2035–1885 Ma Kuandian Group (Meng et al. 2013, 2014), Eastern Liaoning terrain (Zhang 1988). In the Inner Mongolia block, there is a 200 km long Paleoproterozoic phosphorite belt; it includes all the deposits in Hohhot, Jining, Fengzhen, and Hunyuanyao, etc. (Zhu 1982; Yang et al. 2014). In North Korea, the Macheonayeong Series and Nangnim Group (Li et al. 1994) also have economic metamorphic phosphorites (Table 12.1).

In Udaipur region of NW India, there are wave-brecciated stromatolite-bearing phosphorites in early Proterozoic Aravalli Group (∼2.15 Ga, Purohit et al. 2010). The Aravalli Group contains two distinct phosphate-bearing horisons and huge reserves of rock phosphate. The lower phosphorite horizon is more or less close to the base of the Aravalli Group and well known for several important phosphorite deposits, i.e., Jhamar Kotra (50 milliontons with 15–39 % of P_2O_5, 16 million tons with $P_2O_5 > 30$ %), Maton (9.2 million tons with P_2O_5 16–26 %), Dakan Kotra, Kararia-Ka-Gurha, and Kanpur (the latter three with P_2O_5 contents varying from 12 to 25 %). The upper horizon comprises the small phosphorite deposits of Sismarma, Nimach Mata, and Baragaon, with P_2O_5 content ranging from 5 to 23 %. In addition, phosphorus ores are also found in Indian Khondalite series, coexisting with rocks bearing Mn-garnet (Zhu 1982).

In Finland, the U-bearing phosphatic sediments have been found within the supracrustal series metamorphosed during the Svecokarelian Orogeny about 1900–1850 Ma ago, deposited during 2080–1900 Ma (Karhu 1993; Melezhik and Fallick 1996).

Khondalite series in Scandinavian Peninsula, Ceylon (Sri Lanka), North Korea, Russia and Madras and East Ghats of India abound with phosphorus ores (Ji and Chen 1990; Jiang 1990; Lu et al. 1996). Phosphorites about 2000 Ma occur at Rum Jungle in northern Australia, in the Marquette Range of Michigan (phosphoritic pebbles in conglomerates), the Hamersley Group of W Australia and at Broken Hill in SE Australia (Schneider et al. 2002; Bekker et al. 2010; and references therein).

Phosphorites precipitate in strong oxidizing condition because phosphorus should exist as PO_4^{3-} (P^{5+}) in water. Intense biotic agency is another important factor resulting in the formation of phosphorites (e.g., Zhang et al., 2015). Global devoid of Archean phosphorus deposit suggests weak biologic activities and low oxygen fugacity of sedimentary environment before 2300 Ma. On the contrary, widespread development of phosphorites after 2300 Ma suggests a condition with prevailed biomass activities and high oxygen fugacity.

12.2.3 Fast Global Development of the Lake Superior-Type Banded Iron Formations and Record in NCC

It was statistic that more than 90 % of iron ores developed at Precambrian (Isley and Abbott 1999; Shen et al. 2006). Most of those iron ores are banded iron formations (BIFs) and prosperously developed during the period of 2500–1850 Ma (Trendall and Blockley 1970; Trendall 2002). Furthermore, most resource of iron is concentrated on a few Precambrian

superlarge deposits, which are giant sizes (up to 1.0×10^8 Mt for a single deposit, Huston and Logan 2004) and have unique geological features and genesis. Most of the deposit types are not (or few) developed any more at later geological history and nearly disappear at Mesoproterozoic. And just a few BIFs are developed during "Snowball Event" of ca. 800 Ma (Gaucher et al. 2008; Frei et al. 2009; Bekker et al. 2010).

It is considered that the development of BIFs reflected the comprehensive coupling results from both geological tectonic and environmental geochemistry evolutions, as well as organism activities of earth early history (Frei et al. 2008). Precambrian BIFs are generally classified into the Algoma- and Lake Superior-types (Gross 1980, 1983) and mainly formed in Paleoproterozoic when the fO_2 in seawater was high enough to oxidize Fe^{2+} into Fe^{3+} to form voluminous BIFs (Huston and Logan 2004). The Algoma-type BIFs are dominant magnetite (F_3O_4), minor pyrite and devoid of hematite, deposited under reducing conditions with a P_{O2} (partial pressure of oxygen) less than 10^{-65} atm (1 atm = 1.01325×10^5 Pa) (calculated by Garrels et al. 1973). They are mainly developed in the Archean-Paleoproterozoic volcanic–sedimentary formation and associated with greenstone belts (Zhang et al. 2012), represented by the BIFs in the Abitibi greenstone belts (Isley and Abbot 1999). The Lake Superior type BIFs are dominated by hematite (Fe_2O_3) and deposited in oxidic milieu. They were mainly developed in Paleoproterozoic clastic-carbonate formation and associated with the stable sedimentary basins and cratonic margins (Huston and Logan 2004), e.g., the lake superior area of Canada, the Hamersley area of Australia, the Carajas area of Brazil, and the Krivoy Rog area of Ukraine are all the famous source areas of numerous world-class superlarge BIFs (Trendall 2002).

The Hamersley BIFs is 2500 m in thickness and extent up to 4×10^4 km^2 and developed between 2480 and 2450 Ma (Pickard, 2002). It is over 35.6 billion tons in size and more than 24 billion ton rich ores with grade of 50–69 % (Trendall and Morris 1983). The Krivoy Rog Series, Ukranian Shield, is well known BIF-bearing succession. The Sksagan Suite ore field, producing about 85 % of the Krivoy Rog basin output, has the greatest commercial importance. The sedimentation time of Krivoy Rog Series is bracket in 2.6–1.9 Ga, most likely in the range of 2.3–2.0 Ga. Kursk Group marked as Kursk Magnetic Anomaly and composed of metamorphic rocks, is a major iron formation of the Voronezh Massif (Goodwin 1991), Russian, having 42.6 billion tons of iron ores with grade of 32–62 %, including ca. 26.1 billion tons of 54–62 %, and most likely developed during 2300–2000 Ma (Alexandrov 1973). The Karelian Complex (or Supergroup), widely distributed in the eastern part of the Baltic Shield, especially in Russian Karelia and Finland, may serve as a world stratotype of Paleoproterozoic.

Overlying uncomformly on Archean greenstone-granite belt dated at 2800–2600 Ma (granite), it comprises upward the Tunguda-Nadvoitsa, Sariolian (with tillite), Segozero, Onega (BIF, dolomite, stromatolites), Bessovets, and Vepsian (with red bed) Groups (Salop 1977). Metamorphic minerals from the Karelian Complex and syn-Karelian Orogeny granites yield an age of 1900 Ma by different isotopic methods. Therefore, the Karelian Complex is bracket in range 2600–1900 Ma. Carbonate rocks of the Onega Group have been dated at 2300 ± 120 Ma by the Pb-isochron method, while the pre-tectonically intrusive basic dikes give a Pb-isotopic and K–Ar age of 2000–2150 Ma (cf. Salop 1977), suggesting at least the upper portion of the Karelian Complex sedimentated during 2300–2150 Ma. Significant hematite ores are found in the Onega Group which is up to 2000 m in thickness.

The Kaniapiskau Supergroup in the Labrador Trough, Canada is well known of Sokoman BIFs (Dimroth 1981), possessing more than 20.6 billion tons of ores. Dimroth (1981) divided it into three major stratigraphic units, from bottom to top, i.e., the Red Bed Basins (Chakonipau Formation), the Cycle I, and the Cycle II (including the Sokoman BIFs). Because a Rb–Sr isochron of 2.3 Ga has been obtained from volcanics of the easternmost Cape-Smith belt older than the Labrador Trough, Dimroth (1981) suggests the Labrador Trough is of Paleoproterozoic age and younger than 2.3 Ga. A Rb–Sr isochron age of 1.85 Ga for low-grade shales and a K–Ar age also of 1.85 Ga may place the major metamorphism of the Labrador Trough into the Penokean Orogeny that occurred during 1850 Ma, roughly contemporaneous with the Hudson Orogeny assumed to terminate at about 1800 Ma in the rest of the Circum-Superior Belt. However, the age of Kaniapiskau Supergroup is also controversial, for example, Trendall and Morris (1983) argued to be 2400–1800 Ma.

Lake Superior Region including Minnesota, Michigan, and Wisconsin is the most important iron-producing areas in USA, where the BIFs are hosted in Animike Series. The region has shipped 4.6 billion metric tons since 1848. In 1978, the region produced 75 million metric tons of ore or 89 % of the total ore produced in USA and 10 % of the total produced in the world (Morey and Southwick 1995). The Animike Series still contain vast resources; it has been estimated that more than 271 billion metric tons of crude iron ore or 36 billion metric tons of iron-ore concentrate are recoverable (Morey and Southwick 1995). The Animike Series experienced the Penokean Orogeny at about 1850 Ma (Bayley and James 1973; Goodwin 1991) and accumulated during 1930–1850 Ma (Morey and Southwick 1995; Schneider et al. 2002; Canfield 2005). As well known for Homestake Au–Fe formation, the BIFs in the northern Rocky Mountains were confined in Paleoproterozoic

sediments of 2500–1650 Ma, and possibly deposited during 2300–2100 Ma because they were also suggested to be consistent with those in Lake Superior area.

Discovered in 1967, the Carajas iron deposit in Brazil possesses no less than 16 billion tons of high-grade ores (>64 % Fe, averaged at 66.7 %) (Tolbert et al. 1971). Ores were accumulated in the Carajas layer itabirites (iron quartzites) which experienced the Trans-Amazonian Orogeny occurred in the period of 2100–1750 Ma (Goodwin 1991) and is dated around 2000 Ma. The high-grade ores (>60 %) of Itabira Group of Minas Supergroup in the Quadrilatero Ferrifero (Iron Quadrangle) district, Brazil, are estimated to exceed 10×10^9 tons (Goodwin 1991). The Minas Supergroup unconformably covers the granitoid dated of 2500 Ma, and is intruded by pegmatites dated at 2080 Ma (Rb–Sr) as well as the large Cristais pluton dated at 2050 Ma (Rb–Sr) (Goodwin 1991). The Gandarela formation carbonate, under Minas Supergroup, yielded a 2420 ± 19 Ma Pb–Pb isotope age (Babinski et al. 1995). Detrital zircons from a metagreywacke at the top of the Minas Supergroup provide a U–Pb date of 2125 ± 4 Ma (Goodwin 1991). Supporting minimum dates from sphene and zircon in pegmatite intrusion plays the main metamorphism of the Minas Supergroup between 2060 and 2030 Ma. In Guiana Shield, BIFs in Trans-Amazonian greenstone belts are dated at about 2250 Ma (Windley 1983; Klein and Ladiera 2000).

Iron ores in the Singhbhum district, India, bracketed in the period of 2700–2100 Ma, most possible age of 2200–2100 Ma, or of 2300 Ma (Goodwin 1991), are similar with Lake Superior type BIF. The Aravalli Group (~ 2.15 Ga) in NW India has Lake Superior type BIFs, in addition to phosphorite, manganese, copper, uranium deposits (Sreenivas et al. 2001; Ray et al. 2003; Purohit et al. 2010). The Transvaal Supergroup (up to 1.0×10^8 Mt, Trendall and Morris 1983) and correlated Griqualand West Supergroup iron deposits of South Africa were formed at 2480–2322 Ma (Bekker et al. 2001).

It is needed to mention that the pre-GOE Ga BIFs are mainly Algoma-type whereas the post-GOE Ga BIFs are dominated by Lake Superior type. The size of Superior Lake type BIF Fe deposits generally range 10^5–10^8 Mt, far larger than the Algoma-type of 10^3–10^7 Mt (Huston and Logan, 2004). The development time and geological characteristics of these two contrasting types of BIFs strongly demonstrate that the geological environment was rapidly changed during 2.33–2.06 Ga. After 1800 Ma, BIFs were relatively absent and far less in sizes and commercial value than those of pre-1800 Ma. And those intimate related with volcanics are called Rapidan-type BIFs (Gaucher et al. 2008; Frei et al. 2009), which are called volcanic hydrothermal fluid type or volcano rock type in China, while those less related with volcanism or volcanics are named Xinyu type (in South China) or Xuanlong type (in North China).

In China, Algoma-type BIFs are called Anshan type iron ores, and mainly distributed in the Anshan-Benxi area, Liaoning Province, Eastern Hebei, and the North Shanxi Provinces. Those BIFs are mostly hosted in the Neo-Archean volcanic–sedimentary sequences (Zhai et al. 1990; Shen et al. 2005; Zhai 2010; Zhai et al. 2010; Wan et al. 2012; Zhang et al. 2012; Zhai and Santosh 2013), their ore genesises, deposital sizes, and potential prospections, as well as the distributions of BIFs in space and time are closely related to the development of green rock belt. However, most world-class superlarge BIFs belong to the Lake Superior type. Where are the Lake Superior type BIF deposits in China? It is one of important suspended issues for research on iron ore resource of Chinese.

Recently, the 2.38–2.21 Ga Paleoproterozoic Yuanjiachun iron deposit in Lvliang area, Shanxi Province, NCC, has been identified as a representative Lake Superior type BIF in NCC (Fig. 12.1, Table 12.1; Zhu and Zhang 1987; Shen et al. 2010; Zhang et al. 2012; Wang et al. 2015a, b, c; see detail in Chap. 13 and references therein). Another example is the 2.7–1.85 Ga Paleoproterozoic Huoqiu iron deposit belt in Huoqiu area, Anhui Province, it has also been identified as a Lake Superior type BIF (Figs. 12.1, 12.2; Table 12.1; Yang et al. 2014; Liu and Yang 2013, 2015; and references therein). In Laizhou-Anqiu iron deposit belt, Jiaodong Peninsula of eastern China, the Paleoproterozoic BIF deposits in Changyi area have some geological and geochemical characteristics similar to the Superior Lake type BIF (Lan et al. 2012, 2014a, b; 2015). At the southern margin of the NCC, the Tieshanmiao, Hupanling, Malou, Tieshanling iron deposits in "Lushan Group" (Upper Taihua Group) were formed after or at about 2300 Ma (Chen et al. 1996; Wan et al. 2006; Yang 2008; Diwu et al. 2010; Li et al. 2013b; Shen and Song 2014; and references therein). Potential prospections of the Lake Superior type BIFs would be deserved expectation in those areas.

12.2.4 Early Paleoproterozoic Boron Mineralization in NCC

According to incomplete statistics, it has $\sim 46.41 \times 10^6$ tons boron explored reserves in China (The ministry of Land and Resources P.R.C The ministry of Land and Resources P.R.C 2001), and about 91 % production of boron each year comes from Mg-rich borate deposits in Liaoning-Jilin area, NCC (Liu 1996, 2006; Figs. 12.1, 12.2, 12.3; Table 12.1).

The Liao-Ji giant boron belt is a world-class nonmetallic ore province and distributes at the Dashiqiao-Fengcheng-kuangdian area. It trends near east–west direction and about 300 km length and 100 km width with more than 100 large to small size deposits or ore spots, including large-sized boron deposits such as the Houxianyu ore (szaibelyite) in

Fig. 12.3 The stratigraphic units of the Liaohe Group in the Jiao-Liao-Ji Belt (see Tang et al. 2013b, and references therein). Data source of ages from Sun et al. (1993) and Wan et al. (2006)
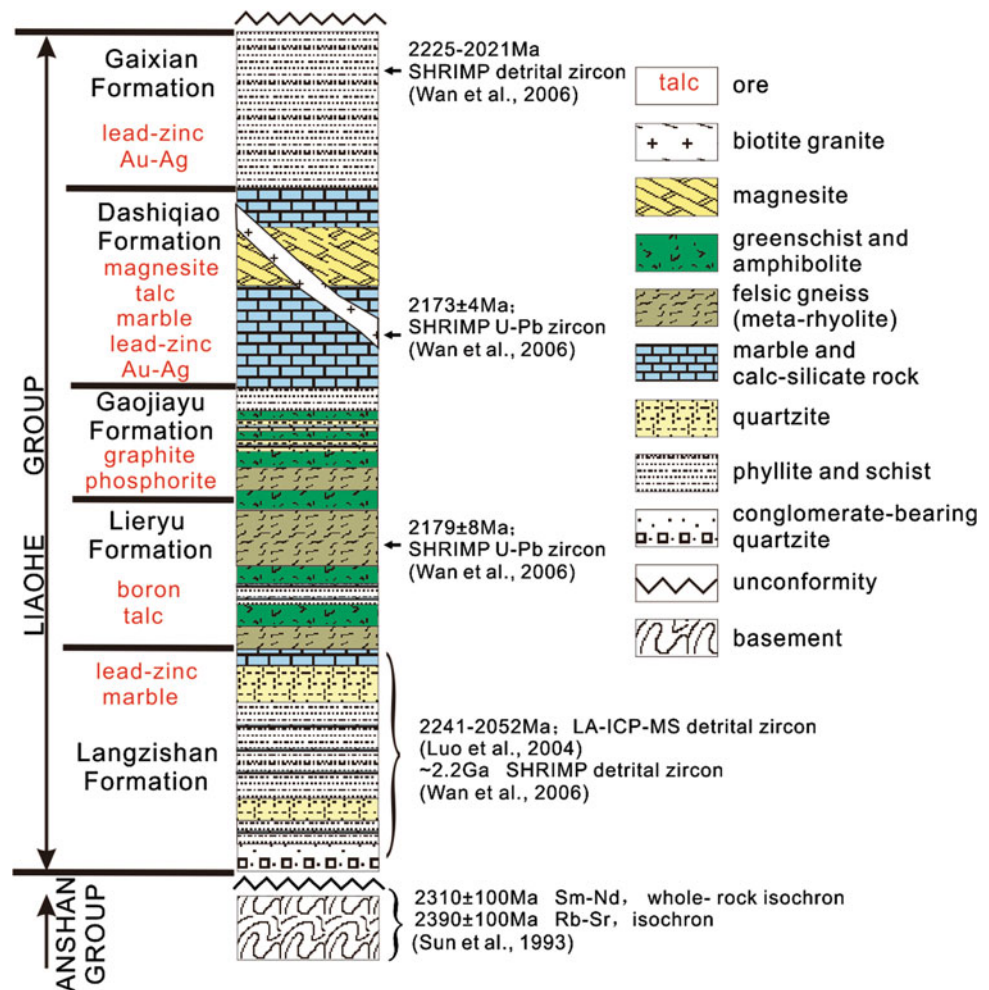
Dashiqiao city, Wengquangou ore (Ludwigite) in Fengcheng city, and Zhuanmiao ore (szaibelyite + ludwigite) in Kuandian area (Figs. 12.1, 12.2; Table 12.1; Qu et al. 2005). Boron ore-bodies mainly hosted in banding magnesite-marbles or near-banding serpentinized Mg-olivine rocks (Feng and Zou 1994; Feng et al. 1998).

These deposits are hosted in the early Paleoproterozoic Lieryu Formation (developed before 2179 Ma, Wan et al. 2006, Li et al. 2015a), Liaohe Group (Jiang et al. 1997, 2004; Xiao et al. 2003; Tang et al. 2009a), which underwent several times intense regional metamorphisms during about 1930–1850, 1450–1400, 885, 386.5, 250–220 Ma (for details see Tang et al. 2009a; and references therein). For example, phlogopite grains yield $^{40}Ar/^{39}Ar$ plateau age of 1918 ± 113 Ma, of 1918 ± 219 separated from the Zhuanmiao deposit, and $^{40}Ar/^{39}Ar$ plateau age of 1923 ± 115 Ma, isochron age of 1924 ± 215 Ma from the Wengquangou deposit, respectively (Lu et al. 2005). Pb–Pb-isochron ages for minerals are 1902 ± 12 Ma of the Zhuanmiao and 1852 ± 9 Ma of the Wenquangou deposits, respectively. These data recorded about 1930–1850 Ma

regional metamorphisms in Liao-Ji giant boron belt, which responded to the Columbia supercontinent aggregation event (Zhao et al. 2004, 2005, 2012; Wan et al. 2015; Liu et al. 2015a; and references therein).

Carbon isotopes of Mg-rich marbles from hosting-rock of boron deposits (Gaojiayu Formation) exhibit clearly positive $\delta^{13}C$ anomalies. For example, the $\delta^{13}C$ of magnesit marbles from the Er'rengou boron deposit are $+3.8 - +5.2$ ‰ (4.8 ± 0.6 ‰, $n = 5$), and those of dolomitic marbles from the (Wang et al. 2008) Luanjiagou boron deposit are $+4.6 - +5.6$ ‰ (5.0 ± 0.4 ‰, $n = 6$). It shows that the Palaeoproterozoic Lieryu Formaton boron-bearing rock series in Liao-Ji area, NCC, records the global GOE.

12.2.5 Early Paleoproterozoic Magnesit Deposits in NCC

In China, world-class magnesit deposits are mainly distributed in the Jiao-Liao-Ji Belt (2.2–1.9 Ga, Li et al. 2015a; Liu et al. 2015a; and references therein) of the NCC

Fig. 12.4 The stratigraphic units of the Fengzishan Group in the Jiao-Liao-Ji Belt (modified after Li et al. 2013a, and references therein). Data source of ages from Shan et al. 2015; Lan et al. 2014a, b; 2015; Xie et al. 2014; and our unpublished paper
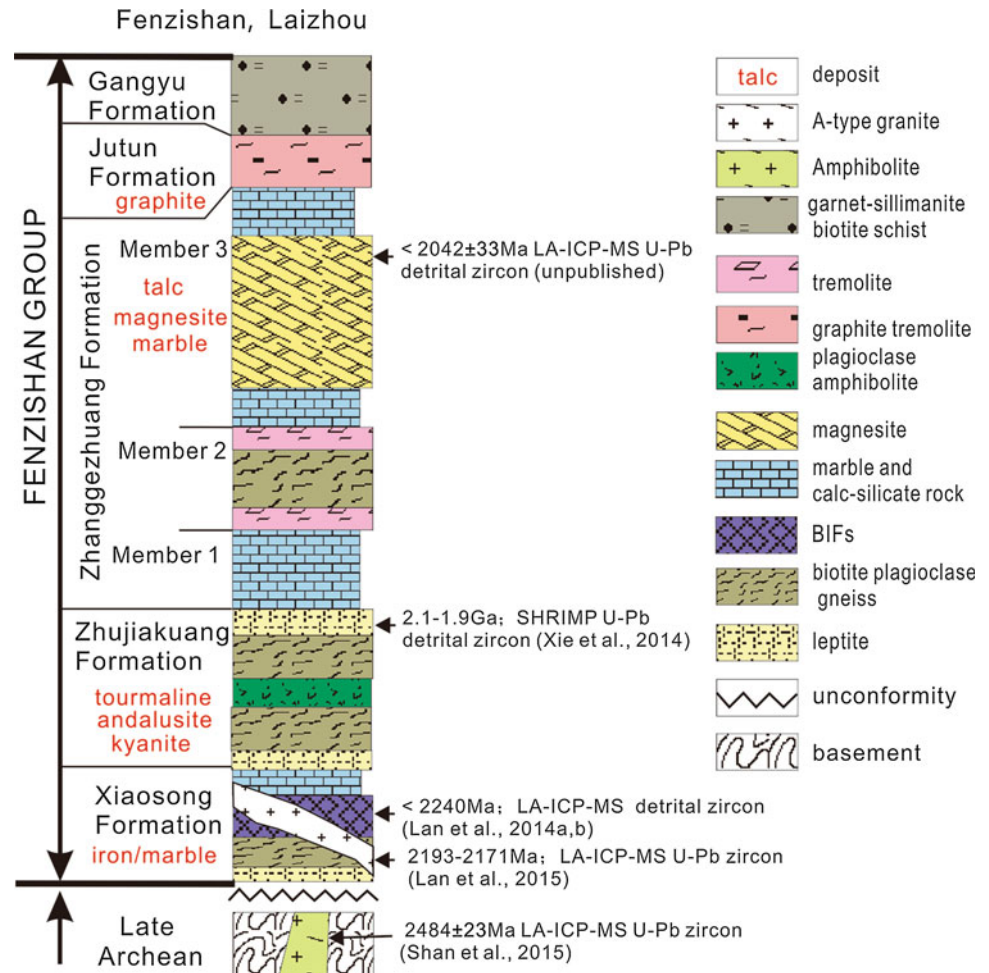
(Figs. 12.1, 12.2, 12.3, 12.4; Table 12.1). A number of important magnesite deposits, including the Shengshuishi, Qingshanhuai, Shuiquan, Huaziyu, Pailou, Jinjiabao, Xiafangsheng, and Fanjiabaozi deposits (Table 12.1; Tang et al. 2013a), occur in the Dashiqiao magnesite belt (Fig. 12.1), and are mainly located in the Haicheng and Dashiqiao counties, Liaoning Province. These deposits are controlled by the third member of the Dashiqiao Formation with bedded or lens-type occurrence, and comprise an important part of the 2.2–2.174 Ga Dashiqiao strata (Jiang et al. 2004; Wan et al. 2006; Tang et al. 2013a), Liaohe Group (2.2–1.9 Ga, Li et al. 2015a,b), in the northeastern NCC. The proven reserve of magnesite in this belt is 2.987 billion tons (The ministry of Land and Resources P.R.C 2001), accounting for >80 % of the total magnesite reserves in China and up to 30 % of the world reserves (Chen et al. 2003a). The Dashiqiao magnesite belt has been an important topic for the IGCP443 (International Geology and Environment Comparison of Magnesite and Talc) project (Chen and Cai 2000; Chen et al. 2003b; Jiang et al. 2004). Carbon and oxygen isotopes from magnesite orebody, hosting-rock (dolomitic marble) of this belt exhibit clearly positive δ^{13}C

anomalies (Tang et al. 2013a; and references therein), it is estimated that the primary sediments of the Dashiqiao Formation might possess δ^{13}C values of >4.2 ‰, and δ^{18}O values of >21.5 ‰. These Palaeoproterozoic carbonate strata, therefore records the global GOE. The formation of the Dashiqiao magnesite deposits involved primary sedimentation (the Palaeoproterozoic evaporate sedimentation in a high-Mg lagoon), diagenesis, regional metamorphism, hydrothermal replacement and local post-ore fluid–rock interaction and records a multistage and polygenetic history (Tang et al. 2013a).

In Jiaodong Peninsula of eastern China, the large Fenzishan magnesit deposit (Figs. 12.1, 12.2, 12.4, Table 12.1) hosted in Paleoproterozoic Zhuanggezhuang Fm., Fenzishan Group (2.1–1.9 Ga; Xie et al. 2014; Tang et al. unpublicated). Carbon isotopes from magnesite orebody, hosting-rock (dolomitic marble) of this deposit are 0.4–2.3 ‰ (1.3 ± 0.6 ‰, n = 30) and also exhibit clearly positive δ^{13}C anomalies (our unpublished data).

The massive sedimentary rocks are mainly sourced from the Paleoproterozoic granitic rocks within the orogenic/mobile belt and the metamorphic basement of the

surrounding ancient blocks, and the protoliths were intensively developed between 2.15 and 1.95 Ga (Liu et al. 2015a).

The massive Palaeoproterozoic sedimentary strata in the Jiao-Liao-Ji Belt, NCC, therefore, record the global GOE.

12.3 Some Problems About Geological Environment Changes and Mineralize Record at 2300 Ma

12.3.1 Formation of Graphite Deposit and Its Time-Controlling

Carbon isotope research has verified that graphite deposit is organogenic, and this suggests that the depositing of ore-bearing formation was accompanied by intense biologic activity (Ji and Chen 1990). Graphite-bearing thin beds had occurred in sedimentary stratum at ca. 2.5 Ga, but graphite deposit is mainly hosted in the strata after 2300 Ma because intense biologic activity occurred only after 2300 Ma. The development of high-grade graphite deposits require that ore-bearing formations must be underwent high-grade metamorphism. Therefore, graphite deposits should be found in the medium–high-grade metamorphic sedimentary formations after 2300 Ma.

We know that Khondalite series are the most favourable host formations, so the margin of NCC and Korean peninsula, where Khondalite series are universally seen, are the most important areas producing graphites.

12.3.2 Occurring Time of Phosphorite and the First Period of Global Phosphorus Deposit

Why did the first period of global phosphorus deposit appear after 2300 Ma? This is because that phosphrite precipitates as phosphate, requiring strong oxidizing condition which at least can assure phosphorus of showing positive five valences. Before 2300 Ma, phosphorus, showing positive five valences, was unstable and merely existed as PH_3 (negative three valences) (indicating supergene condition) because of the reducing supergene environment, at the same time, organic activity was extremely weak and no conditions favourable for the forming of phosphorite were provided, as a result, sedimentary phosphorus ores before 2300 Ma could not be discovered. After 2300 Ma, intense organic activity and formation of the atmosphere rich in oxygen presented some favourable conditions for the depositing phosphorite; thus phosphorite appeared. A lot of PH_3 accumulated in the Earth surface system before 2300 Ma and they suddenly oxidized into phosphate rocks (P^{5+}) after 2300 Ma,

therefore, which led to the first period (2300–1900 Ma) of global phosphorus deposit after 2300 Ma.

It should be mentioned that, the researches of phosphorus deposits of China, Ye (1989) pointed out that formations of phosphorus deposits were related to extraterrestrial factor, and weathering crust viewed extraterrestrial factor as one of three backgrounds of forming the phosphorus deposits. This is consistent with the event at 2300 Ma.

12.3.3 Time-Controlling Rules of Lake Superior Type Iron Deposit

A lot of Fe^{2+} accumulated in the reducing seawater before 2500 Ma. After 2500 Ma, sudden increase of oxygen fugacity resulted in Fe^{2+} being oxidized into Fe^{3+}, and the hydrolysis of Fe^{3+} produced hydroxide precipitates, at last a great number of iron deposits were formed globally, such as Lake Superior area of Canada, Kursk iron ore area of the Soviet Union, and Hamersley area of Australia and so on. Statistical data suggest that Lake Superior type iron deposits account for 60 % of all the iron resources, and 70 % of the rich resources (e.g., Information Division of CAGS 1975; Huston and Logan 2004).

It is obvious that gradualism can never reasonably explain the sudden development of Lake Superior type iron formation during 2500–2300 Ma Siderian and 2050–1800 Ma Orosirian, and why iron formations before 2500 Ma and after 1900 Ma are not so important as those a little after 2500 Ma. This problem would never be understood properly if the event at 2300 Ma had not been recognized scientifically.

12.3.4 Sudden Sedimentation of Carbonates Strata and Related Deposits

Before 2300 Ma, all the continents lacked carbonate rocks, except for some thin-bedded discontinuous carbonate rocks found in very few areas, however, after 2300 Ma, there was a great development of carbonate rocks over the world (Eriksson and Truswell 1978; see Sect. 11.2.3 of Chap. 11). The atmosphere of Archean was rich in CO_2 (e.g., Chen and Zhu 1988), but why were carbonates absent before 2300 Ma? It is generally explained as follows: in the Archaeozoic, weak organic activity and photosynthesis and high CO_2 partial pressure resulted in the reaction $CaCO_3 + CO_2 + H_2O \rightarrow Ca^{2+} + 2HCO_3^-$, and $CaCO_3$ was unstable and uneasy to precipitate (Wang 1989). But after Archean, organic activity increased and photosynthesis consumed a great deal of CO_2, as a result, the reaction $Ca^{2+} + CO_3^{2-} \rightarrow CaCO_3$ occurred. However, this explanation cannot answer the lack of other carbonates strata, such as $FeCO_3$, $MnCO_3$,

and $MgCO_3$, as they can precipitate at high CO_2 partial pressure. Another explanation is that the pH of seawater in Archean was too low to bring about the precipitating a lot of carbonate rocks (e.g., Chen and Zhu, 1985), as carbonate minerals were unstable in acid seawater. The weathering of terrestrial silicate minerals can increase the pH of seawater (Chen 1996a), e.g., $7Na[AlSi_3O_8](Albite) + 26H_2O \rightarrow 3Na_{0.33}Al_{2.33}Si_{3.67}O_{10}(OH)_2$ (Smectite) $+ 10H_4SiO_4$ (Hydrated silica) $+ 6Na^+ + 6OH^-$, $2KAl_3Si_3O_{10}(OH)_2$ (Muscovite) $+ 20H_2O \rightarrow 3Al_2O_3.3H_2O$ (Gibbsite) $+ 2K^+ + 6H_4SiO_4$ (Hydrated silica) $+2OH^-$, and $2Ca[Al_2Si_2O_8]$ (Anorthite) $+ 6H_2O \rightarrow [Al_4Si_4O_{10}](OH)_8$ (Kaolinite) $+ 2Ca^{2+} + 4OH^-$. However, the rate of weathering is slow and cannot explain that the sharp sediment of thick-bedded carbonate strata. The living bloom would be the best answer, with increase of the pH up to some point (see Sect. 12.4), a huge amount of thick-bedded carbonate rocks bearing stromatolites were formed globally (Chen 1990; Chen et al. 1991, 1994).

12.4 Linkage Between Early Paleoproterozoic Metallogenic Explosion in NCC and the GOE

The majority of mineralize records mentioned above (Table 12.1; Figs. 12.1, 12.2, 12.3, 12.4), indicate that there was a 2.5–1.85 Ga early Paleoproterozoic metallogenic explosion in NCC, with the blooms of biogeochemical oxygenic photosynthesis and can be related to the significant atmospheric change events during the GOE. Based on Tang and Chen (2013), Chen and Tang (2016) of Chap. 11 gave a further evolution sequence of these events for ca. 2.5–1.7 Ga Earth's superficial change events, including the widespread deposition of the Siderian banded iron formations (BIFs), slightly postdated by the 2.29–2.25 Ga global Huronian Glaciation Event (HGE, or the oldest Snowball Earth, Kirschvink et al. 2000), then, followed by the development of the 2.22–2.06 Ga carbonate strata with positive $\delta^{13}C_{carb}$ anomalies (Lomagundi/Jatulian Event, see Tang et al. 2004; Tang et al. 2011; and references therein), 2.25–1.95 Ga the oldest red beds in each continents (Melezhik et al. 1997b), as well as the disappearance of BIFs at ca 1.8 Ga and prevalence of black shales at 2.0–1.7 Ga. These significant events, occurred in younging order with somewhat temporal overlap, together with other Earth's superficial changes, resulted from, or relate to the GOE and recorded global changes in the atmosphere, biosphere, hydrosphere, and lithosphere. And the GOE throughout overprinted by the early Paleoproterozoic metallogenic explosion in early Precambrian cratons, such as NCC (Table 12.1; Figs. 12.1; 12.2).

The early Earth's hydrosphere–atmosphere system was obviously anoxic from 4.5 to 2.5 Ga (Cloud 1968, 1973; Holland 1994; Rye and Holland 1998). Such a long anoxic history made the Archaean hydrosphere enriched with a large amount of low-valent ions represented by Fe^{2+}. However, in the geological record, BIFs first appeared at 3.8 Ga but peaked at ca. 2.5 Ga and disappeared at ca. 1.8 Ga (e.g., Klein 2005; Huston and Logan 2004). Experimental simulations (Zhu et al. 2014; and references therein) indicate that the basic requirements for forming BIFs are adequate amounts of Fe^{2+} and the fit seawater pH of 1.25–5.5. If the pH is lower than 1.25, only amorphous colloidal silica would precipitate, no matter whether the solution was heated or not. Therefore, it would precipitate thick layer of siliceous rock rather than BIFs in this period. It suggests an anoxia environment or active volcanism (besides H_2O, the volcanic gas components are acidic gases and reduced gases, including CO_2, H_2, HCl, HF, SO_2, H_2S, CH_4, NH_3, N_2, Cl_2 and others, and H_2 and Cl_2 easily react to form HCl; Chen and Zhu 1985, 1987; Kump and Barley 2007). Otherwise, if the pH is higher than 5.5, silicic acid would highly dissociate and combine with cations to form ferrosilicates (clay minerals, such as black shale or iron-manganese concretion) rather than amorphous silica precipitates (Chen and Zhu 1984; Zhu et al., 2014). In acid seawater ($1.25 < pH < 5.5$) conditions, the precipitation of iron oxide is just opposite to that of amorphous silica. The higher the pH of the solution, the greater iron precipitation can be obtained. But in any case, Fe^{2+} did not precipitate continuously to produce a thick layer of "iron ore" (Zhu et al. 2014). It suggests that the Algoma-type BIFs developed in relative anoxia seawater (meaning low pH near 1.25), while the Superior Lake type BIFs developed in relative oxidic seawater (meaning high pH near 5.5), which was in accordance with the indication of Eu anomalies from Precambrian BIFs (Huston and Logan 2004) or other sediments (Chen and Zhao 1997; Chen et al. 1998; Tang et al. 2013a). And a high pH condition need a more oxidic environment or quiescent times with severer terrestrial weathering, the latter is in accordance with the 2.5–2.3 Ga quiescent time of the Earth (e.g., Condie et al. 2001; Zhai and Santosh 2011, 2013) and the worldwide high CIA values Khondalite series (see previous Sect. 11.3.4). And the former needs biological photosynthesis to give off O_2.

Based on records and discuss mentioned above, as well as Chen and Tang (2016) in Chap. 11, Here we give a summary of framework to explain the relation between early Paleoproterozoic era (2.5–1.8 Ga) metallogenic explosions, such as in NCC, and 2.5–1.7 Ga Earth's superficial change events during the GOE and shown in Fig. 12.5:

1. Since the beginning of the Palaeoproterozoic era, biological photosynthesis was enhanced (Melezhik et al.
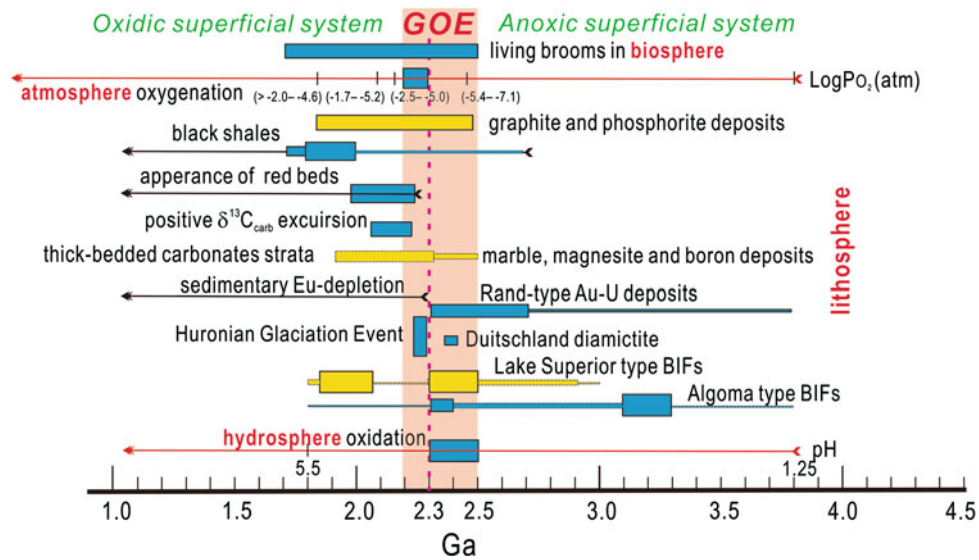
Fig. 12.5 A summary framework for ca. 2.5–1.7 Ga Earth's superficial changes events and metallogenic explosion during the GOE (modified after Tang and Chen 2013; Chen and Tang 2016 in Chap.11 and Tang et al. unpublished). References: pH of seawater (Zhu et al. 2014); Algoma and Lake Superior types BIFs (Huston and Logan 2004); Huronnian Glaciation Event (HGE, Tang and Chen 2013); Rand-type Au-U deposits (Bekker et al. 2005; and references therein); sedimentary Eu-depletion (Tang et al. 2013a); thick-bedded carbonates strata (Eriksson and Truswell 1978); positive $\delta^{13}C_{carb}$ excursion (Karhu and Holland 1996); red beds (see Melezhik et al. 1997a; Bekker et al. 2005; and references therein); black shales (Condie et al. 2001); PO$_2$ in the Paleoproterozoic (Kanzaki and Murakami 2016), other ores see references in text for data source

1997a, b; Chen et al. 2000a; this paper), which fiercely transferred CO$_2$ into organic debris and release O$_2$; the O$_2$ was consumed in oxidation of the accumulated Fe^{2+}, CH$_4$ and elevated the pH value of seawater in the ways of $4Fe^{2+} + O_2 + 4H^+ \rightarrow 4Fe^{3+} + 2\,H_2O$, and $CH_4 + 2O_2 \rightarrow CO_2 + 2H_2O$, as well as $O_2 + H_2O + 4e^- \rightarrow 4OH^-$. During these processes, organic debris was deposited (graphite and phosphorite deposits, organism in black shale, even oil resources), and Lake Superior type BIFs were deposited (e.g., Huston and Logan 2004; Frei et al. 2008; Wang et al. 2015a, b, c), as well as atmospheric CO$_2$ drawdown occurred, CH$_4$ was eliminated (Fig. 12.5).

2. After removal of the majority of reducing components from the oceans which is indicated by widespread deposition of BIFs (Bekker et al. 2010; Tang and Chen 2013), the O$_2$ produced by biological photosynthesis gradually began to accumulate in atmosphere with the devoid of Rand-type Au–U deposits. The 2.29–2.25 Ga global Huronian Glaciation Event slightly postdated the widespread deposition of the Siderian BIFs (mainly Lake Superior type BIFs, Fig. 12.5), due to the icehouse effect of O$_2$ instead of greenhouse effect of CO$_2$ and CH$_4$ (Tang and Chen 2013). And the 0.8–0.6 Ga Snowball Earth was also after algal rise (Feulner et al. 2015).

3. The HGE was followed by widespread deposition of 2.22–2.06 Ga carbonates with positive $\delta^{13}C_{carb}$ anomalies due to the fixation of ^{12}C in organic debris and the

CO$_2$ in hydrosphere–atmosphere system was relatively enriched in ^{13}C (Lomagundi/Jatulian Event, Schidlowski et al. 1975; Schidlowski 1988; Karhu and Holland 1996; Tang et al. 2011; Lai et al. 2012; Salminen et al. 2013). And the oldest red beds in each continent appeared during 2.25–1.95 Ga (Melezhik et al. 1997a).

4. At the same time, with the rise of pH in seawater, those carbonates can began to precipitate in the ways of $CO_2 + 2OH^- \rightarrow CO_3^{2-} + H_2O$, $CO_3^{2-} + Fe^{2+} \rightarrow FeCO_3(\downarrow)$ (Siderite), $CO_3^{2-} + Mg^{2+} \rightarrow MgCO_3(\downarrow)$(Magnesite), $2CO_3^{2-} + Ca^{2+} + Mg^{2+} \rightarrow CaMg\,(CO_3)_2\,(\downarrow)$ (Dolomite), $CO_3^{2-} + Ca^{2+} \rightarrow CaCO_3(\downarrow)$(Calcite), $CO_3^{2-} + Mn^{2+} \rightarrow MnCO_3(\downarrow)$ (Rhodochrosite) etc., as these minerals are unstable in acid seawater (e.g., Chen and Zhu 1985). So, there had been a worldwide sudden sedimentation of carbonate strata and related carbonate deposits (e.g., marble, boron, and magnesite deposits with graphite, phosphorite, and Lead-Zinc deposits in NCC; Figs. 12.1, 12.2, 12.3, 12.4, 12.5) during the 2.3–1.9 Ga (e.g., Chen et al. 2000a; Tang et al. 2009c, 2013b; see previous sections in this paper). And the CO$_2$ in atmosphere rapidly entered into biosphere (organics), hydrosphere (CO_3^{2-}, HCO_3^-) and lithosphere (carbonates), thereby sharply decline.

5. With the O$_2$ was accumulated in the hydrosphere, the majority of the low-valent ions in the oceans were oxidation (e.g., $Fe^{2+} \rightarrow Fe^{3+}$), the pH value of seawater

further elevated ($O_2 + H_2O + 4e^+ \rightarrow 4OH^-$). Gradually, when the pH raised high enough (pH > 5.5), the two basic requirements for forming BIFs (adequate amounts of Fe^{2+} and the fit seawater pH of 1.25–5.5, Zhu et al. 2014) would be not available (Fig. 12.5). Consequently, the BIFs disappear ca. 1.8 Ga (Klein 2005).

6. As for the 2.0–1.7 Ga "black shale", succeeding the withdraw of the BIFs and early Paleoproterozoic carbonate strata (Melezhik et al. 1997a; Condie et al. 2001), its high CIA indexes and contained varying amounts of organic carbon (Condie et al. 2001) indicated that the provenance of black shale underwent severely weathering and long distance transport, and the sedimentation was under an peace with plenty living active environment, which might be the product of ferrosilicates precipitation (clay minerals) with terrestrial weathered materials (see Sect. 12.3.4) and organic remains deposited at higher pH (>5.5, means more oxidic condition) seawater (Fig. 12.5), as these shale showed negative Eu anomalies (Condie 1993; Chen and Zhao 1997; Chen et al. 1998).

12.5 Concluding Remarks

The geology and geochronology of numerous ores, including graphite, phosphorite, the Lake Superior type BIFs, marble, boron, magnesite, and Lead-Zinc deposits, hosted in 2.5–1.8 Ga stata from the NCC and elsewhere, have been complied in this paper. It indicated that there has an early Paleoproterozoic metallogenic explosion in NCC.

The early Paleoproterozoic metallogenic explosion is resulted from the significant Earth's environmental change related to the blooms of biogeochemical oxygenic photosynthesis in biosphere (graphite, phosphorite deposits), which result in hydrosphere (pH increase with dissolved element oxidation from low into high valences, e.g., Lake Superior type BIFs, REE deposits), atmosphere (e.g., CO_2, CH_4 withdraw and HGE), sedimentary sphere (e.g., BIFs, Glacial diamictite, Carbonates strata, Red beds, Black shales) rapidly changes and brought out the 2.5–1.8 Ga Great Oxygen Event (GOE). Different deposits responded to different stage events of the GOE.

The GOE includes the early-stage hydrosphere oxidation (2.5-2.3 Ga) and the late-stage atmospheric oxygenation (2.3–2.2 Ga). A pre-2.3 Ga reducing hydrosphere prevented atmosphere from oxygenation, because of the consumption of O_2 generated from biological photosynthesis in the oxidation of Fe^{2+} and precipitation of BIFs. After 2.3 Ga, increasing O_2 and decreasing CH_4 and CO_2 cooled the hydrosphere–atmosphere system and resulted in the global Huronian Glaciation Event, which was followed by sudden sedimentation of carbonate strata and $\delta^{13}C_{carb}$ positive excursion (Lomagundi Event), red beds, as well as the disappear of BIFs and prevail of black shales. The biogeochemical oxygenic photosynthesis plays a key role and operates throughout the process.

References

Alexandrov, E. A. (1973). The precabrian banded iron-formations of the Soviet Union. *Economic Geology, 68*(7), 1035–1063.

Awramik, S. M., Schopf, J. W., & Walter, M. R. (1983). Filamentous fossil bacteria from the Archean of western Australia. *Precambrian Research, 20*, 357–374.

Babinski, M., Chemale, F, Jr., & Van Schmus, W. R. (1995). The Pb/Pb age of the Minas Supergroup carbonate rocks, Quadrilátero Ferrífero, Brazil. *Precambrian Research, 72*, 235–245.

Bayley, R. W., & James, H. L. (1973). Precambrian iron-formations of the United States. *Economic Geology, 68*(7), 934–959.

Bekker, A., Karhu, J. A., & Kaufman, A. J. (2006). Carbon isotope record for the onset of the Lomagundi carbon isotope excursion in the Great Lakes area, North America. *Precambrian Research, 148*, 145–180.

Bekker, A., Kaufman, A. J., Karhu, J. A., Beukes, N. J., Swart, Q. D., Coetzee, L. L., & Eriksson, K. A. (2001). Chemostratigraphy of the Paleoproterozoic Duitschland Formation, South Africa: Implications for coupled climate change and carbon cycling. *American Journal of Science, 301*, 261–285.

Bekker, A., Kaufman, A. J., Karhu, J. A., & Eriksson, K. A. (2005). Evidence for Paleoproterozoic cap carbonates in North America. *Precambrian Research, 137*, 167–206.

Bekker, A., Slack, J. F., Planavsky, N., Krapež, B., Hofmann, A., Konhauser, K. O., & Rouxel, O. J. (2010). Iron formation: the sedimentary product of a complex interplay among mantle, tectonic, oceanic, and biospheric processes. *Economic Geology, 105*, 467–508.

Canfield, D. E. (2005). The early history of atmospheric oxygen: homage to Robert M. Garrels. *Annual Review of Earth and Planetary Sciences, 33*, 1–36.

Cao, R.-J. (2003). History and current status of study on stromatolitic nomenclature and classification in the Precambrian. *Geological Survey and Research, 26*(2), 80–83 (in Chinese with English abstract).

Cao, R.-J., & Yuan, X.-L. (2009). Advances of stromatolite study in China. *Acta Palaeontologica Sinica, 48*(3), 314–321 (in Chinese with English abstract).

Cao, R.-J., Zhao, W.-J., & Xiao, Z.-Y. (1982). Subdivision and correlation of the Precambrian in China. In: Nanjing Institute of Geology and Paleontology (Ed.), *Stratigraphic correlation chart in China with explanatory text* (pp. 1–27). Beijing: Science Press (in Chinese).

Cenki, B., Braun, I., & Bröcker, M. (2004). Evolution of the continental crust in the Kerala Khondalite Belt, southernmost India: evidence from Nd isotope mapping, U–Pb and Rb–Sr geochronology. *Precambrian Research, 134*(3–4), 275–292.

Chen, Y.-J. (1990). Evidences for the catastrophe in geologic environment at about 2300 Ma and the discussions on several problems. *Journal of Stratigraphy, 14*, 178–186 (in Chinese with English abstract).

Chen, F. (1996a). Origin and evolution of the Earth's atmosphere and hydrosphere. In G.-Z. Tu & Z.-Y. Ouyang (Eds.), *Developments in geochemistry* (pp. 225–233). Guizhou: Guizhou Science and Technology Publishing House (in Chinese).

Chen, Y.-J. (1996b). Progresses in application of sedimentary trace element geochemistry to probe crustal composition and environmental change. *Geology Geochemistry, 3*, 1–125 (in Chinese).

Chen, J. (2002). The black shale series and ore deposit in Qingchengzi Liaoning Province. *Geology and Resources, 11*(3), 188–192 (in Chinese with English abstract).

Chen, C.-X., & Cai, K.-Q. (2000). Minerogenic system of magnesian nonmetalliic deposits in early Proterozoic Mg-rich carbonate formations in eastern Liaoning Province. *Acta Geologica Sinica, 74*, 623–631.

Chen, Y.-J., & Deng, J. (1993). REE geochemical characteristics and evolution of early Preambrian sediments: Evidence from the southern margin of the northern China craton. *Geochimica, 1*, 93–104 (in Chinese).

Chen, Y.-J., & Tang, H.-S. (2016). The Great Oxidation Event and its records in North China Craton. In M.-G. Zhai, et al. (Eds.), *Main Tectonic Events and Metallogeny of the North China Craton* (pp. xx–xx). Singapore: Springer.

Chen, Y.-J., Hu, S.-X., & Lu, B. (1998). Contrasting REE geochemical features between Archean and Proterozoic khondalite series of North China Craton. Goldschmidt Conference Toulouse 1998. *Minralogical Magzine, 62A*, 318–319.

Chen, Y.-J., Ji, H.-Z., Zhou, X.-P., & Fu, S.-G. (1991). The challenge to the traditional geological theories from revelation of the catastrophe at 2300 Ma: New knowledge on several important geological subjects. *Advance in Earth Science, 6*(2), 63–68 (in Chinese with English abstract).

Chen, C.-X., Jiang, S.-Y., Cai, K.-Q., & Ma, B. (2003a). Metallogenic conditions of magnesite and talc deposits in early Proterozoic Mg-rich carbonate formations, eastern Liaoning province. *Mineral Deposits, 22*(2), 166–176 (in Chinese with English abstract).

Chen, Y.-J., Liu, C.-Q., Chen, H.-Y., Zhang, Z.-J., & Li, C. (2000). Carbon isotope geochemistry of graphite deposits and ore-bearing khondalite series in North China: Implications for several geoscientific problems. *Acta Petrologica Sinica, 16*, 233–244 (in Chinese with English abstract).

Chen, C.-X., Ni, P., Cai, K.-Q., Zhai, Y.-S., & Deng, J. (2003b). The minerogenic fluids of magnesite and talc deposits in the Paleoproterozoic Mg-rich carbonate formations in eastern Liaoning Province. *Geological Review, 49*(6), 646–651 (in Chinese with English abstract).

Chen, Y.-J., Ouyang, Z.-Y., Yang, Q.-J., & Deng, J. (1994). A new understanding of the Archean-Proterozoic boundary. *Geologic Review, 40*, 483–488 (in Chinese with English abstract).

Chen, Y.-J., & Su, S.-G. (1998). Catastrophe in geological environment at 2300 Ma. *Mineralogical Magazine, 62A*(1), 320–321.

Chen, Y.-J., Yang, J.-Q., Deng, J., Ji, H.-Z., Fu, S.-G., Zhou, X.-P., & Lin, Q. (1996). An important change in Earth's evolution: An environmental catastrophe at 2300 Ma and its implications. *Geology-Geochemistry, 3*, 106–128 (in Chinese).

Chen, Y.-J., & Zhao, Y. C. (1997). Geochemical characteristics and evolution of REE in the Early Precambrian sediments: Evidences from the southern margin of the North China Craton. *Episodes, 20*, 109–116.

Chen, F., & Zhu, X.-Q. (1984). Simulating experiments on the mechanism of formation of banded iron–silica formation: Weathering–leaching of basalts. *Geochimica, 4*, 341–349 (in Chinese with English abstract).

Chen, F., & Zhu, X. Q. (1985). pH-evolution of Archaean seawater and its relations to ore deposition. *Acta Sedimentologica Sinica, 3*, 1–15 (in Chinese with English abstract).

Chen, F., & Zhu, X.-Q. (1987). The evolution of supergene weathering and its ability of oreforming elements. *Geochimica, 4*, 341–350 (in Chinese with English abstract).

Chen, F., & Zhu, X.-Q. (1988). Reconstruction of evolution of atmospheric CO_2 partial pressure based on the sediment mineral assemblage. *Science China- Earth Sciences, 7*, 747–755 (in Chinese).

Cloud, P. E. (1968). Atmospheric and hydrospheric evolution on the primitive earth. *Science, 160*, 729–736.

Cloud, P. E. (1973). Paleoecological significance of banded iron-formation. *Economic Geology, 68*, 1135–1143.

Cloud, J. P. E., & Semikhatov, M. A. (1969). Proterozoic stromatolite zonation. *American Journal of Science, 267*(9), 1017–1061.

Condie, K. C. (1993). Chemical composition and evolution of the upper continental crust: contrasting results from surface samples and shales. *Chemical Geology, 104*, 1–37.

Condie, K. C., DesMarais, D. J., & Abbott, D. (2001). Precambrian superplumes and supercontinents: A record in black shales, carbon isotopes, and paleoclimates? *Precambrian Research, 106*, 239–260.

Cook, P. J., & Mcelhinny, M. W. (1979). A reevaluation of the spatial and temporal distribution of sedimentary phosphate deposits in the light of plate tectonics. *Economic Geology, 74*, 315–330.

Davidson, C. F. (1963). Phosphate deposits of Precambrian age. *Mining Mag., 109*, 205–342.

Dimroth, E. (1981). Labrador Geosyncline: Type example of early Proterozoic cratonic reactivation. In: A. Kroner (Ed.), *Precambrian Plate Tectonics* (pp. 1–238).

Diwu, C.-R., Sun, Y., Lin, C.-L., & Wang, H.-L. (2010). LA-(MC)-ICP-MS U-Pb zircon geochronol-ogy and Lu–Hf isotope compositions of the Taihua complex on the southern margin of the North China Craton. *Chinese Science Bulletin, 55*, 2557–2571.

Diwu, C.-R., Sun, Y., Yuan, H.-L., Wang, H.-L., Zhong, X.-P., & Liu, X.-M. (2008). The U–Pb chronology of detrital zircon of quartzite and its geological significance of Songshan, Denfeng area of Henan Province. *Chinese Science Bulletin, 53*(16), 1923–1934 (in Chinese).

Du, L.-L., Yang, Z.-H., Lu, Z.-L., Zhao, L., Geng, Y.-S., Diwu, C.-R., et al. (2015). The Sijizhuang Formation at Jiangcun Area of Wutai Mountains: Further Constraints on the Age of the Hutuo Group. *Acta Geoscientica Sinica, 36*(5), 599–612 (in Chinese with English abstract).

Duan, X.-X., Liu, J.-M., Wang, Y.-B., Zhou, L.-L., Li, Y.-G., Li, B., et al. (2012). Geochronology, geochemistry and geological significance of Late Triassic magmatism in Qingchengzi orefield Liaoning. *Acta Petrologica Sinica, 28*(2), 595–606 (in Chinese with English abstract).

Eriksson, K. A., & Truswell, J. F. (1978). Geological process and atmospheric evolution in the Precambrian. In D. H. C. Tarling (Ed.), *Evolution of the Earth's Crust* (pp. 219–238). London: Academic Press.

Feng, B.-Z., Lu, J.-W., Zou, R., Ming, H.-L., & Xie, H.-Y. (1998). Ore-forming conditions for the early proterozoic large-superlarge boron deposits in Liaoning and Jilin Provinces, China. *Journal of Changchun University of Science and Technoly, 28*(1), 1–15 (in Chinese with English abstract).

Feng, X.-Z., Xiao, Y., & Liu, C.-X. (2008). Geology and geochemistry of the Gaotaigou boron deposit in southern Jilin China. *Geology of Chemical Minerals, 30*(4), 207–217 (in Chinese with English abstract).

Feng, B.-Z., & Zou, R. (1994). The characteristics and genesis of Houxianyu doron deposits, Yinkou Liaoning Province. *Earth Science Frontiers, 1*(3–4), 235–237 (in Chinese with English abstract).

Feulner, G., Hallmann, C., & Kienert, H. (2015). Snowball cooling after algal rise. *Nature Geoscience, 8*(9), 659–662. doi:10.1038/ngeo2523.

Frei, R., Dahl, P. S., Duke, E. F., Frei, K. M., Hansen, T. R., Frandsson, M. M., & Jensen, L. A. (2008). Trace element and isotopic characterization of Neoarchean and Paleoproterozoic iron formations in the Black Hills (South Dakota, USA): Assessment of chemical change during 2.9–1.9 Ga deposition bracketing the 2.4–2.2Ga first rise of atmospheric oxygen. *Precambrian Research, 162*, 441–474.

Frei, R., Gaucher, C., Poulton, S. W., & Canfield, D. E. (2009). Fluctuations in Precambrian atmospheric oxygenation recorded by chromium isotopes. *Nature, 461*, 250–253.

Fu, M.-Y. (2014). The prospecting direction of the graphite deposit in Hebei Province. *China Non-metallic Minerals Industry, 109*, 50–52 (in Chinese with English abstract).

Gao, W.-Y., Li, J.-H., Bai, X., & Mao, X. (2009). Structural characterister of a huge Paleoproterozoic stromatolite in Mt. Wutai and its genetic implication. *Acta Petrologica Sinica, 25*(3), 667–674 (in Chinese with English abstract).

Garrels, R. M., Perry, E. A. Jr., & Mackenzie, F. T. (1973). Genesis of Precambrian Iron-formation and the development of atmospheric oxygen. *Economic Geology, 68*, 1173–1179.

Gaucher, C., Blanco, G., Chiglino, L., Poiré, D., & Germs, G. J. B. (2008). Acritarchs of Las Ventanas Formation (Ediacaran, Uruguay): Implications for the timing of coeval rifting and glacial events in western Gondwana. *Gondwana Research, 13*, 488–501.

Goodwin, A. M. (1991). *Precambrian Geology* (pp. 1–521). London: Academic Press.

Gross, G. A. (1980). A classification of iron formations based on depositional environments. *Can. Mineral., 18*, 215–222.

Gross, G. A. (1983). Tectonic systems and the deposition of iron-formation. *Precambrian Research, 20*, 171–187.

Guo, J.-H., Zhai, M.-G., & Li, Y.-G. (1994). Isotopic ages and their tectonic significance of metamorphic rocks from middle part of the early Precambrian granulite belt, North China craton. In X.-L. Qian & R.-M. Wang (Eds.), *Geological evolution of the granulite terrain in north part of the North China Craton* (pp. 130–144). Beijing: China Seismological Press (in Chinese with English abstract).

Holland, H. D. (1994). Early Proterozoic atmospheric change. In: S. Bengston (Ed.), *Early Life on Earth. Nobel Symposium No. 84* (pp. 237–244). New York: Columbia University Press.

Holland, H. D. (2009). Why the atmosphere became oxygenated: A proposal. *Geochimica et Cosmochimica Acta, 73*, 5241–5255.

Hu, S.-X. (1988). *Geology and metallogeny of the collision belts between the Southern and the Northern China Plate* (pp. 1–558). Nanjing: Nanjing University Press (in Chinese).

Hu, G.-Y., Li, Y.-H., Fan, R.-L., Wang, T.-H., Fan, C.-F., & Wang, Y.-B. (2014). The formaiton age of the borate deposit in Kuandian area, eastern Liaoning Province: Constrains from the SHRIMP U–Pb data and boron istopic composition. *Acta Geologica Sinica, 88*(10), 1932–1943.

Hu, S.-X., Zhao, Y.-Y., Xu, J.-F., & Ye, Y. (1997). *Geology of gold deposits in North China platform* (pp. 7–55). Beijing: China Science Press (in Chinese).

Huston, D. L., & Logan, G. A. (2004). Barite BIFs and bugs: Evidence for the evolution of the Earth's early hydrosphere. *Earth Planetary Science Letters, 220*, 41–55.

Information Division of CAGS. (1975). Selections of overseas geologic data (20) (pp. 1–200). Unpublished (in Chinese).

Isley, A. E., & Abbott, D.H. (1999). Plume-related mafic volcanism and the deposition of banded iron formation. *Journal of Geophysical Resarch. B: Solid Earth Planets* 104, 15461–15477.

Ji, H.-Z., & Chen, Y.-J. (1990). Khondalite series and their related mineral resources. *Geology and Prospecting, 11*, 11–13 (in Chinese).

Jiang, S.-Y. (1988). Stable isotope geological characteristics of Oxygen, Carbon, Lead, and Sulfur and metllogenesis of the Qingchengzi Lead-Zinc deposit Liaoning. *Geologic Review, 34*(6), 515–523 (in Chinese with English abstract).

Jiang, J.-S. (1990). Khondalite series and its research progress. *Journal of Changchun University of Earth Sciences, 20*(2), 167–176 (in Chinese with English abstract).

Jiang, S.-Y., Chen, C.-X., Chen, Y.-Q., Jiang, Y.-H., Dai, B.-Z., & Ni, P. (2004). Geochemistry and genetic model for the giant magnesite deposits in the eastern Liaoning province China. *Acta Petrologica Sinica, 20*(4), 765–772.

Jiang, S.-Y., Palmer, M.-R., Peng, Q.-M., & Yang, J.-H. (1997). Chemical and stable isotopic compositions of Proterozoic metamorphosed evaporites and associated tourmalines from the Houxianyu borate deposit, eastern Liaoning, China. *Chemical Geology, 135*, 189–211.

Jiang, S.-Y., & Wei, J.-Y. (1989). Geochemistry of the Qingchengzi Lead-Zinc deposit. *Mineral Deposits, 8*(4), 20–28 (in Chinese with English abstract).

Kanzaki, Y., & Murakami, T. (2016). Estimates of atmospheric O_2 in the Paleoproterozoic from paleosols. *Geochimica et Cosmochimica Acta, 174*, 263–290.

Karhu, J. A. (1993). Palaeoproterozoic evolution of the carbon isotope ratios of sedimentary carbonates in the Fennoscandian Shield. *Geological Survvey of Finland Bulletin, 371*, 1–87.

Karhu, J. A., & Holland, H. D. (1996). Carbon isotopes and the rise of atmospheric oxygen. *Geology, 24*(10), 867–870.

Kirschvink, J. L., Gaidos, E. J., Bertani, L. E., Beukes, N. J., Gutzmer, J., Maepa, L. N., & Steinberger, R. E. (2000). Paleoproterozoic snowball Earth: Extreme climatic and geochemical global change and its biological consequences. *Proceedings of the National Academy of Sciences of the United States of America, 97*, 1400–1405.

Klein, C. (2005). Some Precambrian banded iron-formations (BIFs) from around the world: their age, geologic setting, mineralogy, metamorphism, geochemistry, and origin. *American Mineralogist, 90*, 1473–1499.

Klein, C., & Ladiera, E. A. (2000). Geochemistry and petrology of some Proterozoic banded iron-formations of the Quadrilátero Ferrífero, Minas Gerais, Brazil. *Economic Geology, 95*, 205–428.

Knoll, A. H., Strother, P. K., & Rossi, S. (1988). Distribution and diagenesis of microfossils from the lower Proterozoic Duck Creek Dolomite, Western Australia. *Precambrian Research, 38*, 257–279.

Konhauser, K. O., Lalonde, S. V., Planavsky, N. J., Pecoits, E., Lyons, T. W., Mojzsis, S. J., et al. (2011). Aerobic bacterial pyrite oxidation and acid rock drainage during the Great Oxidation Event. *Nature, 478*, 369–373.

Konhauser, K. O., Pecoits, E., Lalonde, S. V., Papineau, D., Nisbet, E. G., Barley, M. E., et al. (2009). Oceanic nickel depletion and a methanogen famine before the Great Oxidation Event. *Nature, 458*, 750–753.

Kump, L. R., & Barley, M. E. (2007). Increased subaerial volcanism and the rise of atmospheric oxygen 2.5 billion years ago. *Nature, 448*, 1033–1036.

Lai, Y., Chen, C., & Tang, H.-S. (2012). Paleoproterozoic positive δ^{13}C excursion in Henan, China. *Geomicrobiology Journal, 29*, 287–298.

Lan, X.-Y. (1981). Study on genesis of the Nanshu graphite deposit and on feature of Precambrian graphite-bearing rock association, Shandong. *Journal of Changchun University of Earth Sciences, 3*, 30–42 (in Chinese with English abstract).

Lan, T.-G., Fan, H.-R., Hu, F.-F., Yang, K.-F., Cai, Y.-C., & Liu, Y.-S. (2014a). Depositional envi-ronment and tectonic implications of Paleoproterozoic BIF in the Changyi area, eastern North China Craton: evidence from geochronology and geochemistry ofwall-rocks. *Ore Geology Reviews, 61*, 52–72.

Lan, T.-G., Fan, H.-R., Hu, F.-F., Zheng, X.-L., & Zhang, H.-D. (2012). Geological and geochemical characteristics of Paleoproterozoic Changyi banded iron formation deposit, Jiaodong Peninsula of eastern China. *Acta Petrologica Sinica, 28*(11), 3595–3611.

Lan, T.-G., Fan, H.-R., Santosh, M., Hu, F.-F., Yang, K.-F., Yang, Y.-H., & Liu, Y.-S. (2014b). U-Pbzircon chronology, geochemistry and isotopes of the Changyi banded iron forma-tion in eastern Shandong Province: Constraints on BIF genesis and implications for Paleoproterozoic tectonic evolution of the North China Craton. *Ore Geology Reviews, 56*, 472–486.

Lan, T.-G., Fan, H.-R., Yang, K.-F., Cai, Y.-C., Wen, B.-J., & Zhang, W. (2015). Geochronology, mineralogy and geochemistry of alkali-feldspargranite and albite granite association from the Changyi area of Jiao-Liao-Ji Belt: Implications for Paleoproterozoic rifting of eastern North China Craton. *Precambrian Research, 266*, 86–107.

Li, Z.-L. (2014). The geological characteristics and utilization prospect of the Jingcun graphite deposit, Pingdu city, Shandong Province. *China Non-metallic Minerals Industry, 112*, 45–46 (in Chinese with English abstract).

Li, Z., Chen, B., Liu, J.-W., Zhang, L., & Yang, C. (2015a). Zircon U–Pb ages and their implications for the South Liaohe Group in the Liaodong Peninsula Northeast China. *Acta Petrologica Sinica, 31*(6), 1589–1605 (in Chinese with English abstract).

Li, N., Chen, Y.-J., McNaughton, N. J., Ling, X.-X., Deng, X.-H., Yao, J.-M., & Wu, Y.-S. (2015b). Formation and tectonic evolution of the khondalite series at the Southern margin of the North China Craton: Geochronological Constraints from a 1.85-Ga Mo deposit in the Xiong'ershan area. *Precambrian Research, 269*, 1–17.

Li, H.-K., Li, Y.-F., Geng, K., Zhuo, C.-Y., Zhang, Y.-B., Liang, T.-T., & Wang, F. (2013a). Palaeoprpterozoic Tectonic Setting in the Eastern Shandong Province. *Geological Survey and Research, 36*(2), 114–130 (in Chinese with English abstract).

Li, Y.-Y., Luo, Y.-Q., Dongye, M.-X., Bi, R.-F., Zhou, M.-J., Wang, C.-W., et al. (1994). Phosphous deposits in China. In: S, H. Song. (Ed.), *Ore deposits of China* (Vol. 3, pp. 1–59). Beijing: China Geological Publishing House (in Chinese).

Li, H.-Q., Sheng, L.-S., & Jia, X.-J. (2012). Study on the Prospecting Direction in the External of Jingshansi Deposit in Wuyang Iron Ore Field Henan Province. *Gold Science & Technology, 20*(1), 54–60 (in Chinese with English abstract).

Li, Y.-F., Xie, K.-J., Luo, Z.-Z., & Li, J.-P. (2013b). Geochemistry of Tieshan iron deposit in the Wuyang area, Henan Province and its environmental implications. *Acta Geoligical Sinica, 87*(9), 1377–1398.

Li, H.-Q., & Zhang, Y.-L. (2011). Evaluation on deep prospecting potential of the iron mountain mine in Wuyang Henan. *Mineral Exploration, 2*(5), 487–493 (in Chinese with English abstract).

Liu, J.-L. (1988). Study on Precambrian geology of the Jiamusi block. *Journal of Changchun University of Earth Sciences, 18*(2), 147–156 (in Chinese with English abstract).

Liu, J.-D. (1996). Geological characteristics and genesis of early Proterozoic borate deposits in east Liaoning-Shouth Jili. *Geology of*

Chemical Minerals, 18(3), 207–212 (in Chinese with English abstract).

Liu, J.-D. (2006). *Mineralization model and survey & evaluation of early Proterozoic Mg-borate deposits in east Liaoning (doctor candidate paper)* (pp. 1–114). Beijing: China University of Geoscience (in Chinese with English abstract).

Liu, Q.-Q., Li, Y.-F., Luo, Z.-C., Xie, K.-J., & Huang, Z.-L. (2014). Geochemical characteristics of Jingshansi iron deposit in Wuyang, Henan Province, and their geological significance. *Mineral Deposits, 33*(4), 697–712 (in Chinese with English abstract).

Liu, P.-H., Liu, F.-L., Wang, F., & Liu, J.-H. (2011). U–Pb dating of zircons from Al-rich paragneisses of Jingshan Group in Shandong peninsula and its geological significance. *Acta Petrologica et Mineralogica, 30*(5), 829–843 (in Chinese with English abstract).

Liu, F.-L., Liu, P.-H., Wang, F., Liu, C.-H., & Cai, J. (2015a). Progresses and overviews of voluminous meta-sedimentary series within the Paleoproterozoci Jiao-Liao-Ji orogenic/mobile belt, Norht China Craton. *Acta Petrologica Sinica, 31*(10), 2816–2846 (in Chinese with English abstract).

Liu, P.-H., Liu, F.-L., Wang, F., Liu, C.-H., Yang, H., Liu, J.-H., et al. (2015b). P-T-t paths of the multiple metamorphic events of the Jiaobei terrane in the southeastern segment of the Jiao-Liao-Ji Belt (JLJB), in the North China Craton: Implication for formation and evolution of the JLJB. *Acta Petrologica Sinica, 31*(10), 2889–2941 (in Chinese with English abstract).

Liu, S.-W., Lv, Y.-J., Feng, Y.-G., Liu, X.-M., Yan, Q.-R., Zhang, C., & Tian, W. (2007a). Zircon and monazite geochronology Hongqiy-ingzi complex, northern Hebei. *China. Geological Bulletin of China, 26*(9), 1086–1100 (in Chinese with English abstract).

Liu, S.-W., Lv, Y.-J., Feng, Y.-G., Zhang, C., Tian, W., Yan, Q.-R., & Liu, X.-M. (2007b). Geology and zircon U–Pb isotopic chronology of Dantazi Complex, Northern Hebei Province. *Geological Journal of China Universities, 13*(3), 484–497 (in Chinese with English abstract).

Liu, J.-Z., Qian, R.-X., & Chen, Y.-P. (1989). The tectonic orgin of graphite deposits in the khondalite group, the middle part of inner Mongolia China. *Geotectonica et Metallogenia, 13*(2), 162–167 (in Chinese with English abstract).

Liu, H.-J., Sha, D.-X., & Li, G.-S. (2013). Genetic connection between the Lead-Zinc and Gold-Silver deposits in the Qingchengzi ore concentration area in eastern Liaoning. *Geology and Resources, 22*(4), 299–303 (in Chinese with English abstract).

Liu, J.-D., Xiao, R.-G., Wang, S.-Z., & Wang, C.-Z. (2005a). Geological characteristics and exploration of Zhuanmiao borate deposit Liaoning Province. *Geology and Resources, 14*(2), 126–131 (in Chinese with English abstract).

Liu, J.-D., Xiao, R.-G., Wang, C.-Z., Zhou, H.-C., & Fei, H.-C. (2005b). Genesis of the Dashiqiao granite and its significance in Borate mineral exploration. *Journal of Jilin University (Earth Science Edition), 35*(6), 714–719 (in Chinese with English abstract).

Liu, L., & Yang, X.-Y. (2013). Geochemical characteristics of the Huoqiu BIF ore deposit in Anhui Province and their metallogenic significance: Taking the Bantazi and Zhouyoufang deposits as examples. *Acta Petrologica Sinica, 29*(7), 2551–2566 (in Chinese with English abstract).

Liu, L., & Yang, X.-Y. (2015). Temporal, environmental and tectonic significance of the Huoqiu BIF, southeastern North China Craton: Geochemical and geochronological constraints. *Precambrian Research, 261*, 217–233.

Liu, C.-H., Zhao, G.-C., Sun, M., Zhang, J., & Yin, C.-Q. (2012). U-Pb geochronology and Hf isotope geochemistry of detrital zircons from the Zhongtiao Complex: Constraints on the tectonic evolution of the Trans-North China Orogen. *Precambrain Research, 222–223*, 159–172.

Lu, Y.-F., Chen, Y.-C., Li, H.-Q., Xue, C.-J., & Chen, F.-W. (2005). Metallogenic chronology study of boron deposits in early protero-zoic rift in east Liaoning. *Acta Geologica Sinica, 79*(2), 287.

Lu, L.-Z., Xu, X.-C., & Liu, F.-L. (1996). *The Early Precambrian khondalite Series in North China* (pp. 1–276). Changchun: Changchun Publishing House (in Chinese).

Luo, Y., Sun, M., Zhao, G.-C., Li, S.-Z., Xu, P., Ye, K., & Xia, X.-P. (2004). LA ICP-MS U-Pb zircon ages of the Liaohe Group in the Eastern Block of the North China Craton: Constraints on the evolution of the Jiao-Liao-Ji Belt. *Precambrian Research, 134*, 349–371.

Lyons, T. W., & Reinhard, C. T. (2009). Early Earth: Oxygen for heavy-metal fans. *Nature, 461*, 179–181.

Maibam, B., Sanyal, P., & Bhattacharya, S. (2015). Geochronological study of metasediments and carbon isotopes in associated graphites from the Sargur area, Dharwar craton: Constraints on the age and nature of the protoliths. *Journal of the Geological Society of India, 85*.

Melezhik, V. A., & Fallick, A. E. (1996). A widespread positive $\delta^{13}C_{carb}$ anomaly at 2.33-2.06 Ga on the Fennoscandian Shield: A paradox? *Terra Nova Research, 8*, 141–157.

Melezhik, V. A., Fallick, A. E., Filippov, M. M., & Larsen, O. (1999a). Karelian shungite–an indication of 2.0-Ga-old metamorphosed oil-shale and generation of petro-leum: geology, lithology and geochemistry. *Earth-Science Reviews, 47*, 1–40.

Melezhik, V. A., Fallick, A. E., Makarikhin, V. V., & Lubtsov, V. V. (1997a). Links between Palaeoproterozoic palaeogeography and rise and decline of stromatolites: Fennoscandian Shield. *Precambrian Research, 82*, 311–348.

Melezhik, V. A., Fallick, A. E., Medvedev, P. V., & Makarikhin, V. V. (1999b). Extreme $^{13}C_{carb}$ enrichment in ca. 2.0 Ga magnesite–stromatolite–dolomite–'red beds' association in a global context: A case for the worldwide signal enhanced by a local environment. *Earth-Science Reviews, 48*, 71–120.

Melezhik, V. A., Fallick, A. E., & Semikhatov, M. A. (1997b). Could stromatolite-forming cyanobacteria have influenced the global carbon cycle at 2300-2060 Ma? *Norges Geologiske Undersøkelse Bulletin, 433*, 30–31.

Meng, E., Liu, F.-L., Cui, Y., Liu, P.-H., Liu, C.-H., & Shi, J.-R. (2013). Depositional ages and tectonic implications for the Kuan-dian South Liaohe Group in Northeast Liaodong Peninsula. *Northeast China. Acta Petrologica Sinica, 29*(7), 2465–2480 (in Chinese with English abstract).

Meng, E., Liu, F.-L., Liu, P.-H., Liu, C.-H., Yang, H., Wang, F., et al. (2014). Petrogenesis and tectonic implications of Paleoproterozoic meta-mafic rocks from central Liaodong Peninsula, Northeast China: Evidence from zircon U–Pb dating and in situ Lu-Hf isotopes, and whole-rock geochemistry. *Precambrian Research, 247*, 92–109.

Morey, G. B., & Southwick, D. L. (1995). Allostratagraphic relation-ships of Early Proterozoic iron-formations in the Lake Superior region. *Economic Geology, 90*, 1983–1993.

Peng, Q.-M., Palmer, M. R., & Lu, J.-W. (1998). Geology and geochemistry of the Paleoproterozoic borate deposits in Liaoning-Jilin, northeastern China: Evidence of metaevaporites. *Hydrobiologia, 381*, 51–57.

Pickard, A. L. (2002). SHRIMP U-Pb zircon ages of tuffaceous mudrocks in the Brockman Iron Formation of the Hamersley Range, Western Australia. *Australian Journal of Earth Sciences, 49*, 491–507.

Purohit, R., Sanyal, P., Roy, A. B., & Bhattacharya, S. K. (2010). 13C enrichment in the Palaeoproterozoic carbonate rocks of the Aravalli Supergroup, northwest India: Influence of depositional environment. *Gondwana Research, 18*, 538–546.

Qu, H.-X., Guo, W.-J., Zhang, Y., Tan, W.-G., Chen, S.-L., Li, Q.-L., & Bian, X.-F. (2005). Genesis study and prospective prediction for boron deposits in eastern Liaoning. *Geology and Resoures, 14*(2), 131–138 (in Chinese with English abstract).

Ray, J. S., Veizer, W. J., & Davis, (2003). C, O, Sr and Pb isotope systematics of carbonate sequences of the Vindhyan Supergroup, India: Age, diagenesis, correlations and implications for global events. *Precambrian Research, 121*, 103–140.

Rui, Z.-Y., Li, N., & Wang, L.-S. (1991). *Lead and zinc deposits of Guanmenshan* (208 pp). Beijing: Geological Publishing House (in Chinese with English abstract).

Rye, R., & Holland, H. D. (1998). Paleosols and the evolution of atmospheric oxygen: A critical review. *American Journal of Science, 298*, 621–672.

Salop, L. J. (1977). *Precambrian of the northern hemisphere* (pp. 1–378). Amsterdam: Elsevier Press.

Salminen, P. E., Karhu, J. A., Melezhik, V. A. (2013). Tracking lateral δ13Ccarb variation in the Paleoproterozoic Pechenga Greenstone Belt, the north eastern Fennoscandian Shield. *Precambrian Research, 228*, 177–193.

Sanyal, P., Acharya, B. C., Bhattacharya, S. K., Sarkar, A., Agrawal, S., & Bera, M. K. (2009). Origin of graphite, and temperature of metamorphism in Precambrian Eastern Ghats Mobile Belt, Orissa, India: A carbon isotope approach. *Journal of Asian Earth Sciences, 36*(2–3), 252–260.

Satish-Kumar, M., Yurimoto, H., Itoh, S., & Cesare, B. (2011). Carbon isotope anatomy of a single graphite Crystal in a metapelitic migmatite revealed by high-spatial resolution SIMS analysis. *Contributions to Mineralogy & Petrology, 162*(4), 821–834.

Schidlowski, M. (1988). A 3800-million-year isotopic record of life from carbon in sedimentary rocks. *Nature, 333*, 313.

Schidlowski, M., Eichmann, R., & Junge, C. E. (1975). Precambrian sedimentary carbonates: carbon and oxygen isotope geochemistry and implications for the terrestrial oxygen budget. *Precambrian Research, 2*, 1–69.

Schneider, D. A., Bickford, M. E., Cannon, W. F., Schulz, K. J., & Hamilton, M. A. (2002). Age of volcanic rocks and syndepositional iron formations, Marquette Range Supergroup: Implications for the tectonic setting of Paleoproterozoic iron formations of the Lake Superior region. *Canadian Journal of Earth Sciences, 39*, 999–1012.

Schopf, J. W. (1977). Evidences of Archean life. In C. Ponnamperuam (Ed.), *Chemical evolution of the early Precambrian* (pp. 101–105). New York: Academic Press.

Shan, H.-X., Zhai, M.-G., Oliveira, E. P., Santosh, M., & Wang, F. (2015). Convergent margin magmatism and crustal evolution during Archean-Proterozoic transition in the Jiaobei terrane: Zircon U–Pb ages, geochemistry, and Nd isotopes of amphibolites and associated grey gneisses in the Jiaodong complex, North China Craton. *Precambrian Research, 264*, 98–118.

Shen, Q.-H., & Song, H.-X. (2014). Redefiniton of the Taihua Group, Lushan. *Hunan. Journal of stratigraphy, 38*(1), 1–7 (in Chinese with English abstract).

Shen, B.-F., Zhai, A.-M., Miao, P.-S., Sima, X.-Z., & Li, J.-J. (2006). Geological character and potential resources of iron deposits in the North China block. *Geological Survey and Research, 29*(4), 244–325 (in Chinese with English abstract).

Shen, B.-F., Zhai, A.-M., & Yang, C.-L. (2010). Paleoproterozoic animportant metallogenic epoch in China. *Geoligical Survey and Research, 33*(4), 241–256 (in Chinese with English abstract).

Shen, B.-F., Zhai, A.-M., Yang, C.-L., & Cao, X.-L. (2005). Temporal–spatialdistribution and evolutional characters of Precambrian iron deposits in China. *Geological Survey and Research, 28*(4), 196–206 (in Chinese with English abstract).

Sreenivas, B., Sharma, D. S., Kumar, B., Patil, D. J., Roy, A. B., & Srinivasan, R. (2001). Positive $\delta^{13}C$ excursion in carbonate and organic fractions from the Paleoproterozoic Aravalli Supergroup, Northwestern India. *Precambrian Research, 106*, 277–290.

Sun, M., Armstrong, R. L., Lambert, R. S., Jiang, C.-C., & Wu, J.-H. (1993). Petrochemistry and Sr, Pb and Nd isotopic geochemistry of Paleoproterozoic Kuandian Complex, the eastern Liaoning Province, China. *Precambrian Research, 62*, 171–190.

Sun, H.-J., Wu, C.-L., & Qu, Y.-Y. (1995). Khondalite and graphite deposits from Liaohe Group. *Mineral Resources and Geology, 9*(3), 208–212 (in Chinese with English abstract).

Tang, H.-S., & Chen, Y.-J. (2013). Global glaciations and atmospheric change at ca. 2.3Ga. *Geoscience Frontiers, 4*, 583–596.

Tang, G.-J., Chen, Y.-J., Huang, B.-L., & Chen, C.-X., (2004). Paleoprotoerozoic $\delta^{13}C_{carb}$ positive excursion event: research progress on 2. 3 Ga catastrophe. *Journal of Mineralogy and Petrology 24*(3), 103–109 (in Chinese with English abstract).

Tang, H.-S., Chen, Y.-J., Santosh, M., & Yang, T. (2013a). REE geochemistry of carbonates from the Guanmenshan Formation, Liaohe Group, NE Sino-Korean Craton: Implications for seawater compositional change during the Great Oxidation Event. *Precambrian Research, 227*, 316–336.

Tang, H.-S., Chen, Y.-J., Santosh, M., Zhong, H., Wu, G., & Lai, Y. (2013b). C–O isotope geochemistry of the Dashiqiao magnesite belt, North China Craton: implications for the Great Oxidation Event and ore genesis. *Geological Journal, 48*, 467–483.

Tang, H.-S., Chen, Y.-J., & Wu, G. (2009a). ^{40}Ar-^{39}Ar dating and its geological implication of the Houxianyu boron deposit Liangning province. *Acta Petrologica Sinica, 25*(11), 2752–2762 (in Chinese with English abstract).

Tang, H.-S., Chen, Y.-J., Wu, G., & Yang, T. (2009b). Rare earth element geochemistry of carbonates of Dashiqiao Formation, Liaohe Group, eastern Liaoning province: Implications for Lomagundi event. *Acta Petrologica Sinica, 25*(11), 3075–3093 (in Chinese with English abstract).

Tang, H.-S., Wu, G., & Lai, Y. (2009c). The C-O isotope geochemistry and genesis of the Dashiqiao magnesite deposit, Liaoning province, NE China. *Acta Petrologica Sninca, 25*(2), 455–467 (in Chinese with English abstract).

Tang, H.-S., Chen, Y.-J., Wu, G., & Lai, Y. (2008). The C–O isotope composition of the Liaohe Group, northern Liaoning province and its geologic implications. *Acta Petrologica Sinica, 24*(1), 129–138 (in Chinese with English abstract).

Tang, H.-S., Chen, Y.-J., Wu, G., & Lai, Y. (2011). Paleoproterozoic positive $\delta^{13}C_{carb}$ excursion in northeastern Sino-Korean craton: evidence of the Lomagundi Event. *Gondwana Research, 19*, 471–481.

The ministry of Land and Resources P.R.C. (2001). *Reporting the Land and Resources of China in 2000* (pp. 1–157). Beijing: Geological Publishing House (in Chinese).

Tolbert, G. E., Tremaine, J. W., Melcher, C. C., & Gomes, C. B. (1971). The recently discovered Serra dos Carajas iron depositsNorthern Briazil. *Economic Geology, 66*(7), 895–994.

Trendall, A. F. (2002). The significance of iron-formation in the Precambrian stratigraphic record. *Special Publications International Association of Sedimentology, 33*, 33–66.

Trendall, A. F., & Blockley, J. G. (1970). The iron formations of the Precambrian Hamersley Group, Western Australia with special reference to the crocidolite. *Geological Survey of Western Australia Bulletin 119*, 366 p.

Trendall, A. F., & Morris, R. C. (Eds.). (1983). *Transvaal Supergroup, South Africa, Iron formation: facts and problems* (pp. 471–490). Amsterdam: Elsevier.

Wan, Y.-S., Dong, C.-Y., Wang, W., Xie, H.-Q., & Liu, D.-Y. (2010a). Archean basement and a Paleoproterozoic collision orogen in the Huoqiu Area at the Southeastern marginof North China Craton: Evidence from sensitive high resolution ion micro-probe U–Pb zircon geochronology. *Acta Geologica Sinica, 84*, 91–104.

Wan, Y.-S., Dong, C.-Y., Xie, H.-Q., Wang, S.-J., Song, M.-C., Xu, Z.-Y., et al. (2012). Formation ages of Early Precambrian BIFs in the North China Craton: SHRIMP zircon U–Pb dating. *Acta Petrologica Sinica, 86*(9), 1447–1478 (in Chinese with English abstract).

Wan, Y.-S., Liu, D.-Y., Wang, S.-Y., Zhao, X., Dong, C.-Y., Zhou, H.-Y., et al. (2009). Early Precambrian crustal evolution in the Dengfeng Area, Henan Province (eastern China): Constraints from Geochemistry and SHRIMP U–Pb Zircon Dating. *Acta Geologica Sinica, 83*(7), 982–999.

Wan, Y.-S., Miao, P.-S., Liu, D.-Y., Yang, C.-H., Wang, W., Wang, H.-C., et al. (2010b). Formation ages and source regions of the Paleoproterozoic Gaofa, Hutuo and Dongjiao groups in the Wutai and Dongjiao areas of the North China Craton from SHRIMP U–Pb dating of detrital zircons: Resolution of debates over their stratigraphic relationships. *Chinese Science Bulletin, 55*(13), 1278–1284.

Wan, Y.-S., Song, B., Liu, D.-Y., Wilde, S. A., Wu, J.-S., Shi, Y.-R., et al. (2006). SHRIMP U-Pb zircon geochronology of Palaeoproterozoic metasedimentary rocks in the North China Craton: evidence for a major Late Palaeoproterozoic tectonothermal event. *Precambrian Research, 149*(3–4), 249–271.

Wan, B., Windly, B. F., Xiao, W.-J., Feng, J.-Y., & Zhang, J.-E. (2015). Paleoproterozoic high-pressure metamorphism in the northern North China Craton and implications for the Nuna supercontinent. *Nature Communications, 6*, 8344. doi:10.1038/ncomms9344.

Wang, S.-Q. (1989). The geological features of host rocks and metallogenesis of the Xinghe graphite deposit Nei Mongol. *Mineral Deposit, 8*(1), 85–96 (in Chinese with English abstract).

Wang, X.-W., & Han, X. (1989). A stady on metallogenic regularity of boron deposits in the Ji'an area, Jilin Province. *Jilin Geology, 1*, 72–76 (in Chinese with English abstract).

Wang, C.-Z., Xiao, R.-G., & Liu, J.-D. (2008). Ore-controlling factors and metallogenesis of borate deposits in eastern Liaoning and Southern Jilin. *Mineral Deposits, 27*(6), 727–741 (in Chinese with English abstract).

Wang, C.-Z., Xiao, R.-G., Liu, J.-D., Fei, H.-C., Wang, W.-W., Zhou, H.-C., & Liu, J.-Q. (2006). Ore control role of ultra_magnesium peridotite in Houxianyu boron ore district, Yingkou Liaoning Province. *Mineral Deposits, 25*(6), 683–692 (in Chinese with English abstract).

Wang, F.-R., & Xue, J.-Q. (2010). Geological characteristics and genesis of Beizi crystal graphite deposit in LusanHenan Province. *Mineral Exploration, 1*(3), 248–253 (in Chinese with English abstract).

Wang, C.-L., Konhauser, K. O., & Zhang, L.-C. (2015a). Depositional Environment of the Paleoproterozoic Yuanjiacun Banded Iron Formation in Shanxi Province, China. *Economic Geology, 110*, 1515–1539.

Wang, C.-L., Zhang, L.-C., Dai, Y.-P., & Lan, C.-Y. (2015b). Geochronological and geochemical constraints on the origin of clastic meta-sedimentary rocks associated with the Yuanjiacun BIF from the Lüliang Complex, North China. *Lithos, 212–215*, 231–246.

Wang, C.-L., Zhang, L.-C., Lan, C.-Y., Li, H.-Z., & Huang, H. (2015c). Analysis of sedimentary facies and depositional environment of the Yuanjiachun banded iron formation in the Lvliang area. *Shanxi Province. Acta Petrologica Sinica, 31*(6), 1671–1693 (in Chinese with English abstract).

Wen, D.-J., & Teng, S.-R. (2014). Preliminary discussion on the geochemical prospecting model for the Wengquangou ironoboron deposit in Liaoning Province. *Geology and Resources, 23*(3), 256–260 (in Chinese with English abstract).

Wilde, S. A., Zhao, G.-C., Wang, K.-Y., & Sun, M. (2004). First precise SHRIMP U-Pb zircon ages for the Hutuo Group, Wutaishan: further evidence for the Palaeoproterozoic amalgamation of the North China Craton. *Chinese Science Bulletin, 49*, 83–90.

Windley, B. F. (1980). Evidence for land emergence in the early to middle Precambrian. *Proceeding of the Geologists Association, 91*, 13–23.

Windley, B. F. (1983). Banded iron formation in Proterozoic greenstone belts: Call for further studies. *Precambrian Research, 20*, 585–588.

Windley, B. F. (1984). The evolving continents (pp. 1–399). Chichester: Wiley (second edition).

Wu, F.-Y., Han, R.-H., Yang, J.-H., Wilde, S. A., Zhai, M.-G., & Park, S. C. (2007a). Initial constrains on the timing of granitic magmatism in North Korea using U–Pb zircon geochronology. *Chemical Geology, 238*(3–4), 232–248.

Wu, C.-H., Li, H.-M., Zhong, C.-T., & Chen, Q.-A. (1998). The ages of zircon and rutile (cooling) from khondalite in Huangtuyao, inner Mongolia. *Geological Review, 44*(6), 618–626 (in Chinese with English abstract).

Wu, C.-L., & Qu, Y.-Y. (1994). The geological characteristics and the genesis of the heigoushi graphite deposit, Huanren county Liaoning Provinces. *Nonmetallic Geology, 74*(4), 25–27 (in Chinese with English abstract).

Wu, C.-H., Sun, M., Li, H.-M., Zhao, G.-C., & Xia, X. P. (2006). LA-ICP-MS U-Pb zircon ages of the khondaites from the Wulashan and Jining high-grade terrain in northern margin of the North China Craton: Constraints on sedimentary age of the khondalite. *Acta Petrologica Sinica, 22*(11), 2639–2654 (in Chinese with English abstract).

Wu, Y.-L., Xie, L.-F., Zhang, Y.-L., Fu, M., Ma, J.-C., & Wang, J.-M. (2011). Geological features and prospecting direction of Quanyan crystalline graphite deposit, Ji'an CityJilin Province. *Jilin Geology, 74*(4), 25–27 (in Chinese with English abstract).

Wu, F.-Y., Yang, J.-H., Wilde, S. A., Liu, X.-M., Guo, J.-H., & Zhai, M.-G. (2007b). Detrital zircon U–Pb and Hf isotopic constraints on the crustal evolution of North Korea. *Precambrian Research, 159* (3–4), 155–177.

Xia, X.-H., & Wei, X.-S. (2005). Comprehensive utilization and its geology of zhaobinggou iron/ phosphate deposit in Fengning Hebei Province. *Geology of Chemical Minerals, 27*(1), 1–5 (in Chinese with English abstract).

Xiao, R.-G., Takao, O., Fei, H.-C., & Nomura, M. (2003). Sedimentary-metamorphic boron deposits and their boron isotopic compositions in eastern Liaoning Province. *Geoscience, 17*(2), 137–142 (in Chinese with English abstract).

Xie, S.-W., Wang, S.-J., Xie, H.-Q., Liu, S.-J., Dong, C.-Y., Ma, M.-Z., et al. (2014). SHRIMP U-Pb dating of detrital zircons from the Fenzhishan Group in eastern Shandong Norht China Craton. *Acta Petrologica Sinica, 30*(10), 2989–2998 (in Chinese with English abstract).

Xie, Z., Zhang, H.-T., Chu, X.-Q., Liu, G.-H., Liu, X.-W., & Zhi, Y.-Q. (2015). The regional metallogenic characteritics and prospecting criteria of boron deposit in Kuandian area of Liaoning province. *Chine Mining Magazine, 24*(8), 79–83 (in Chinese with English abstract).

Yang, C.-X. (2008). Zircon SHRIMP U–Pb ages, geochemical characteristics and environmental evolution of the Early Pr ecambrian metamorphic series in the Lushan area, Henan China. *Geological Bulletin of China, 27*(4), 517–533 (in Chinese with English abstract).

Yang, Q.-Y., Santosh, M., & Wada, H. (2014). Graphite mineralization in Paleoproterozoic khondalites of the North China Craton: A carbon isotope study. *Precambrian Research, 255*, 641–652.

Yang, X.-Y., Wang, B.-H., Du, Z.-B., Wang, Q.-C., Wang, Y.-X., Tu, Z.-B., et al. (2012). On the metamorphism of the Huoqiu Group, forming ages and mechanism of BIF and iron deposit in the Huoqiu region, southern margin if North China craton. *Acta Petrologica Sinica, 28*(11), 3476–3496 (in Chinese with English abstract).

Ye, L.-J. (1989). *Phosphorus deposits of China* (pp. 286–311). Beijing: China Science Press (in Chinese).

Young, G. M. (2012). Secular changes at the Earth's surface: evidence from palaeosols, some sedimentary rocks, and palaeoclimatic perturbations of the Proterozoic Eon. *Gondwana Research, 24*(2), 453–467.

Young, G. M. (2013). Precambrian supercontinents, glaciations, atmospheric oxygenation, metazoan evolution and an impact that may have changed the second half of Earth history. *Geoscience Frontiers, 4*, 247–261.

Cao R.-J., & Yuan, X.-L. (2003). Brief history and current status of stromatolite study in China. *Acta Micropalaeontologica Sinica 20* (1), 5–14 (in English with Chinese abstract).

Zhai, M.-G. (2010). Tectonic evolution and metallogenesis of North China Craton. *Mineral Deposits, 29*(1), 24–36 (in Chinese with English abstract).

Zhai, M.-G., Li, T.-S., Peng, P., Hu, B., Liu, F., Zhang, Y.-B., et al. (2010). Precambrian key tectonic events and evolution of the North China Craton. In: T. M. Kusky, M.-G. Zhai, & W.-J. Xiao (Eds.), *The Evolving Continents: Understanding Processes of Continental Growth* (Vol. 338, pp. 235–262). London: Geological Society of London, Special Publication.

Zhai, M.-G., & Santosh, M. (2011). The early Precambrian odyssey of the North China Craton: A synoptic overview. *Gondwana Research, 20*, 6–25.

Zhai, M.-G., & Santosh, M. (2013). Metallogeny in the North China Craton: Secular changes in the evolving Earth. *Gondwana Research, 24*, 275–297.

Zhai, M.-G., Windly, B. F., & Sills, J. D. (1990). Archean gneisses, amphibolites and banded iron formations from the Anshan area of Liaoning Province, NE China: Their geochemistry, metamorphism and petrogenesis. *Precambrian Research, 46*, 195–216.

Zhang, Q.-S. (Ed.). (1984). Geology and metallogeny of the early Precambrian in China (pp. 536). Jilin Peoples' Press, Changchun (in Chinese with English abstract).

Zhang, Q.-S., (1988). *The early crust evolution and mineral deposits in eastern Liaoning Province Peninsula* (pp. 1–213). Beijing: Geological Publishing House (in Chinese with English abstract).

Zhang, Q.-S. (2013). From Neixiang county, Henan Province, the Wuyangshan mining area graphite mine geology and genesis of ore deposits. *Geology of Chemical Minerals, 35*(3), 175–178 (in Chinese with English abstract).

Zhang, Q., & Liu, S. (2014). Ore deposit features and prospecting criteria of crystalline graphite mine in Ji'an area Jilin Province. *Jilin Geology, 33*(3), 60–62 (in Chinese with English abstract).

Zhang, W., Yang, R.-G., Mao, T., Ren, H.-L., Gao, J.-B., & Chen, J.-Y. (2015). Sedimentary environment and mineralization mechanism of the stromatolitic phosphorite in the Ediacaran Dengying Formation, Weng' an County of Guizhou Province China. *Geological Journal of China Universities, 21*(2), 186–195 (in Chinese with English abstract).

Zhang, H.-F., Zhai, M.-G., Santosh, M., Wang, H.-Z., Zhao, L., & Ni, Z.-Y. (2014a). Paleoproterozoic granulites from the Xinghe graphite mine, North China Craton: Geology, zircon U–Pb geochronology and implications for the timing of deformation, mineralization and metamorphism. *Ore Geology Reviews, 63*, 478–497.

Zhang, L.-C., Zhai, M.-G., Wan, Y.-S., Guo, J.-H., Wang, C.-L., & Liu, L. (2012). Study of the Precambrian BIF-iron deposits in the North China Craton: Progresses and questions. *Acta Petrologica Sinica, 28*(11), 3431–3445 (in Chinese with English abstract).

Zhang, T.-Y., Zhang, Z.-L., & Li, J.-Q. (2014b). Summary of research status on regional metamorphic graphite deposit in China. *China Non-metallic Minerals Industry, 111*, 36–38 (in Chinese with English abstract).

Zhao, D.-X. (1982). The age and genesis of phosphorous deposits of the Dongjiao Type. *Scientia Geologica Sinica, 4,* 386–394 (in Chinese with English abstract).

Zhao, Z.-H. (2010). Banded iron formation and great oxidation event. *Earth Science Frontiers, 17,* 1–12 (in Chinese with English abstract).

Zhao, G.-C., Cawood, P. A., Li, S.-Z., Wilde, S. A., Sun, M., Zhang, J., et al. (2012). Amalgamation of the North China Craton: Key issues and discussion. *Prcambrian Research, 222–223,* 55–76.

Zhao, G.-C., Sun, M., Wilde, S. A., & Li, S.-H. (2004). A Paleo-Mesoproterozoic supercontinent: Assembly, growth and breakup. *Earth-Science Reviews, 67,* 91–123.

Zhao, G.-C., Sun, M., Wilde, S. A., & Li, S.-Z. (2005). Late Archean to Paleoproterozoic evolution of the North China Craton: key issues revisited. *Precambrian Research, 136,* 177–202.

Zheng, Y.-F., Xiao, W.-J., & Zhao, G.-C. (2013). Introduction to tectonics of China. *Gondwana Research, 23,* 1189–1206.

Zhu, S.-Q. (1982). The geological features of the stratiform phosphate deposits of China. *Earth Sciences, 1*:157–166 (in Chinese with English abstract).

Zhu, X.-Q., Tang, H.-S., & Sun, X.-H. (2014). Genesis of banded iron formations: A series of experimental simulations. *Ore Geology Reviews, 63,* 465–469.

Zhu, J.-C., & Zhang, F.-S. (1987). The formation condition of the Precambrian iron ores in Yuanjiachun ore deposit Shanxi Province. *Mineral Deposits, 6*(1), 11–21 (in Chinese with English abstract).